

# Large Amplitude Oscillatory Shear Experiments to Investigate the Nonlinear Viscoelastic Properties of Highly Loaded Carbon Black Rubber Compounds Without Curatives

Jean L. Leblanc

University P. & M. Curie (Paris 6), Polymer Rheology and Processing, 60, rue Auber – F-94408 Vitry-sur-Seine cedex, France

Received 9 August 2007; accepted 19 November 2007

DOI 10.1002/app.28196

Published online 17 April 2008 in Wiley InterScience (www.interscience.wiley.com).

**ABSTRACT:** The nonlinear viscoelastic properties of two series of highly loaded carbon black natural rubber composites with filler volume fraction in the 0.148–0.309 range were investigated at 100°C through strain sweep tests at 0.5 and 1.0 Hz frequency, up to strain amplitude of around 1000%, using a commercial torsional dynamic rheometer adapted to perform so-called Fourier Transform rheometry experiments. A series of high *cis*-1,4 polybutadiene (BR)/carbon compounds with filler fractions in the 0–0.213 range was also tested for comparison. Except BR compounds with carbon black fractions below the so-called percolation level (0.12–0.13), nonlinear viscoelastic responses were systematically observed within the experimental strain window (6–1000%). Fourier Transform treatment of recorded torque and strain signals allowed to express the material response in terms of harmonics, with the main one (i.e., at to the test frequency) corresponding to the complex modulus. The usual drop of complex modulus with increasing strain was

observed and adequately analyzed with a model previously reported. The expected effect of carbon black content was observed. Highly loaded samples were found to exhibit a variation of relative torque harmonics with strain amplitude markedly different from unfilled rubbers, which lead to the development of a model, inspired by the Weibull analysis. This model explicitly considers that filler particles, dispersed in the rubber matrix, self-organize in a structure that adds a nonlinear response to the growing nonlinearity exhibited by the polymer matrix as applied strain increases. Above a critical strain, easily determined by mathematically handling model parameters, the filler structure dislocates and the high strain nonlinear response of the matrix is asymptotically recovered. © 2008 Wiley Periodicals, Inc. *J Appl Polym Sci* 109: 1271–1293, 2008

**Key words:** elastomers; fillers; morphology; rheology; viscoelastic properties

## INTRODUCTION

When loaded with sufficient levels of reinforcing filler, e.g., carbon blacks or high-structured silica, most rubber compounds exhibit peculiar rheological properties whose origin is the self-structuring capability of such materials, imparted by the strong physico-chemical interactions which are occurring between the polymer matrix and dispersed filler particles. Highly loaded rubber compounds are very challenging systems for rheological testing, first because they are far to correspond to the ideal, homogeneous, isotropic material considered when establishing the so-called rheometrical equations (which convert the measured quantities into rheological parameters), second because either due to their stiffness or owing to minor compounding ingredients, actual boundary conditions might be very complicated.

Progress in material science is limited by capabilities of observational and experimental techniques. This common sense statement is particularly true in what the rheology of highly complex polymer systems, such as filled rubber compounds, is concerned. Indeed, while relatively simpler pure polymers may be investigated with quite a number of well spread techniques, it is now recognized that, owing to their excessive stiffness yet in the so-called molten state, filled compounds require rheometers working in pressurized conditions to yield reproducible and meaningful results. Practically this reduces the possible test techniques to only a few ones: the complicated and tedious extrusion rheometry for the high simple shear rate range, the (variable rate) Mooney disk rheometer for the intermediate range and “sandwich” type or sliding cylinder rheometers for the very low shear rate range. Only extrusion rheometers (plunger type capillary testers or instrumented extruders) and single rate Mooney testers are commercially available.

Torsional dynamic rheometers offer another approach, not really involving a net flow situation of

Correspondence to: J. L. Leblanc (jleblanc@ccr.jussieu.fr).

the tested material, but attractive with respect to linear viscoelastic considerations that, in theory, allow the readily measured material response to be split into elastic and viscous components. Unfortunately, the tremendously wide capabilities that open gap rheometers, i.e., parallel disks and cone-and-plate, offer with most pure molten polymers are of very little help in what filled rubber compounds and similar complex materials are concerned, essentially because stiff molten materials cannot be reproducibly positioned in the testing gap. Fortunately, side developments of testing principles initially invented to document the vulcanization behavior of activated rubbers, proved to be an interesting rheometrical approach over the last decades. Indeed, when submitting to a periodic (i.e., sinusoidal) torsional strain a stiff filled compound, tightly maintained in a closed cavity, a reproducible complex stress (or torque) can be measured up to very large deformations, in the 1000% range if the frequency is lower than 0.5 Hz. However, because nonlinear viscoelastic responses are obtained, test results must be treated in the appropriate manner, for instance through the so-called Fourier Transform, as pioneered by Wilhelm.<sup>1</sup>

In the work reported here, highly loaded carbon black rubber compounds without curatives were investigated at the standard test temperature of 100°C through large amplitude oscillatory shear testing, i.e., so-called Fourier Transform rheometry experiments, essentially designed to address the nonlinear viscoelastic response of polymer materials.

## EXPERIMENTAL

### LAOS rheometry with a closed cavity torsional dynamic tester

Even at 100°C, most filled rubber compounds are too stiff to be correctly handled with conventional dynamic rheometers, i.e., cone-plate or parallel disks rheometers. Special instruments are needed, for instance the so-called Rubber Process Analyzer RPA<sup>®</sup> (Alpha Technologies, a division of Dynisco, Akron, USA) or the Moving Die Processability Tester MDpt<sup>®</sup> (TechPro, Akron, USA). These instruments are essentially closed cavity torsional dynamic rheometers, with a reciprocal cones test chamber, whose upper and lower dies are maintained with a closing force of around 16 kN. The appropriate modifications were brought to a RPA, as previously reported in details,<sup>2</sup> to capture strain and torque signals and subsequently perform various data analysis, namely Fourier Transform (FT) calculations. FT is nothing else than a calculation technique that converts a material property observed in the time domain, i.e., the torque signal, into the same property expressed in the frequency domain, i.e., the so-called torque spectrum (Fig. 1). FT analysis of periodic signals yields

### RPA at 100°C; 1 Hz; Strain angle : 20 deg (279.25 %) High cis-1,4 polybutadiene

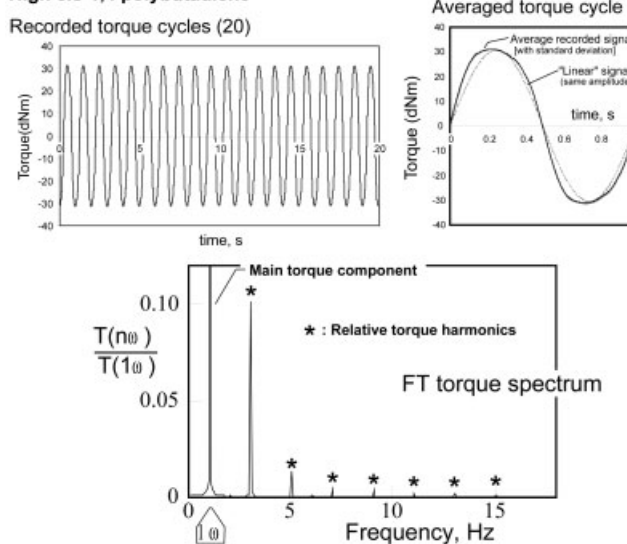


**Figure 1** Typical recorded torque signal when submitting a high *cis*-1,4 polybutadiene sample to a harmonic strain of 20° at 1 Hz frequency; average torque cycle and Fourier Transform spectrum

essentially two types of information: first the main signal component, i.e., the peak in the FT spectrum that corresponds to the applied frequency [hereafter noted either  $T(1\omega)$  or  $S(1\omega)$  with respect to the torque or strain signals, respectively], second the harmonics, with the third (i.e., the peak at  $3\times$  the applied frequency) the most intense one.

Despite the quality design and the care in manufacturing an advanced tester such as the RPA, there are technical limits in accurately submitting test material to sinusoidal strain, well documented, however, by the Fourier Transform analysis of the strain (i.e., applied) signal.<sup>3</sup> Extensive experiments with our RPA-FT instrument have revealed that the applied strain signal is not perfect and that there are significant (i.e., larger than noise) harmonic components in the strain signal, which however decrease with higher strain amplitude, whatever the test conditions, in such a manner that high strain tests are performed in better-applied signal conditions than low strain ones. Because both the applied strain and the measured torque signals are simultaneously FT analyzed, an easy and practical method has been developed to correct for what can be considered as minor (and inevitable) instrument deficiencies. Essentially, relative torque harmonics  $T(n\omega/1\omega)$  data are corrected according to:

$$T(n\omega/1\omega)_{\text{corr}} = T(n\omega/1\omega)_{\text{TF}} - CF_n \times S(n\omega/1\omega)_{\text{TF}} \quad (1)$$

where  $T(n\omega/1\omega)_{\text{TF}}$  and  $S(n\omega/1\omega)_{\text{TF}}$  are the  $n$ th relative harmonic components of the torque and strain signals, respectively, and  $CF_n$  the correction factor,

as derived from a plot of  $T(n\omega/1\omega)$  versus  $T(n\omega/1\omega)$ . Whatever the tested material,  $T(n\omega/1\omega)$  versus  $S(n\omega/1\omega)$  decreases, passes through a minimum and is bounded by a straight line whose slope provides the correction factor. The correction method is based on the simple argument that, if the applied strain were perfect, all  $T(n\omega/1\omega)$  data points would fall on the vertical axis. Detailed demonstrations of this correction method have been reported for the 3rd relative torque harmonic<sup>4</sup> and for the so-called "total torque harmonic content," TTHC, i.e., the sum  $\sum T(n\omega/1\omega)$  of all the odd harmonics up to the fifteenth.<sup>5</sup>

### Testing protocol for nonlinear viscoelastic investigations

High strain dynamic testing is a method of choice to study the nonlinear viscoelastic behavior of polymer materials and an appropriate test protocol was developed with the objectives to document this behavior over a large strain range, while simultaneously obtaining information on the test repeatability and the material quality, in the minimum testing time. This protocol essentially consists in performing strain sweep experiments through two subsequent runs separated by a resting period of 2 min (note: an arbitrary choice, but generally found largely sufficient for viscoelastic recovery with most polymer systems tested so far). At least two samples of the same material are tested (more if results reveal test material heterogeneity), in such a manner that, through inversion of the strain sequences (i.e., run 1 and run 2), sample fatigue effects are detected, if any. Differences are expected between runs 1 and 2 for materials exhibiting strain memory effects, either permanent or at least not fully dampened after 2 min resting period. If the material is of good quality, i.e., homogeneous or well dispersed, results gathered on the two samples superimpose. At each strain sweep step, after a sufficient number of cycles to reach a stable periodic strain situation, data acquisition is made to record 10,240 points at the rate of 512 pt/s. This corresponds to 20 cycles at 1.0 Hz frequency and 10 cycles at 0.5 Hz. With the RPA, the maximum applicable strain angle depends on the frequency, for instance around  $68^\circ$  ( $\approx 950\%$ ) at 0.5 Hz, considerably larger than with open cavity cone-plate or parallel disks torsional rheometers.<sup>6</sup> Whatever the frequency, the lower strain angle limit is  $0.5^\circ$  (6.98%) below which the harmonic content of the strain signal becomes so high that the measured torque is excessively scattered and likely meaningless. Test protocols at 0.5 Hz were designed to probe the material's viscoelastic response within the  $0.5^\circ$ – $68^\circ$  range, with up to 20 investigated strain angles. Test protocols at 1.0 Hz cover the 0.5 to  $33^\circ$  range,

with also 20 strain angles. The maximum strain angle permitted with the RPA is  $90^\circ$ , only possible at very low frequency, for instance 0.1 Hz. However, because on one hand the instrument requires a sufficient number of cycles to reach and stabilize the set angle, and because on the other hand Fourier transform calculation proved to yield good results only if the data acquisition involves several cycles, LAOS experiments performed at frequencies lower than 0.5 Hz result in excessively long testing times and were not considered useful with respect to the objectives of the present work.

### Extra (strain-induced) versus intra (morphology-induced) nonlinear viscoelasticity

When a viscoelastic materials is submitted to high periodic strain, a distorted torque signal is recorded and Fourier Transform allows to express the material response in the frequency domain, through the so-called torque spectrum. Distortions in torque signals are expected to correspond to harmonics appearing at odd multiples of the applied frequency. But experiments with many complex polymer systems, namely filled rubber compounds, have revealed a limit of this data treatment. Whether the torque signal is distorted "on the left" or "on the right," with respect to a vertical axis drawn at the first quarter of the cycle, does not reflect in the FT spectrum. It was observed, moreover, that filled rubber systems exhibit severer distortions, which sometimes affect more the right part of the half signal, when strong interactions can be suspected between components (i.e., phases) of materials (Fig. 2). In other terms,

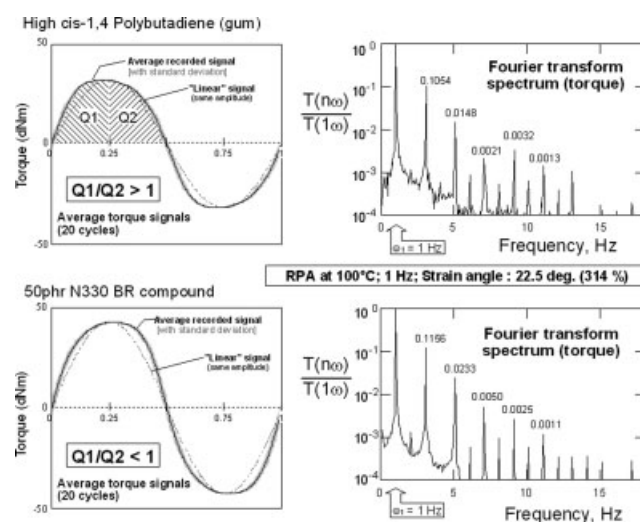


**Figure 2** Recorded torque signals during RPA tests at high strain on a gum and a 50 phr polybutadiene compound; Fourier transform torque spectra; principle of quarter cycle integration technique to document the nonlinear viscoelastic character through  $Q1/Q2$  ratio.



there is a substantial difference between the nonlinear viscoelastic behavior of a pure, unfilled polymer and of a complex polymer material.

By nature, polymers are nonlinear materials, even if under extreme limiting conditions they can exhibit a linear behavior, for instance at very low strain and/or rate of strain. The linear viscoelasticity can be considered as a time induced deviation from a purely elastic behavior, to which strain induced deviation adds to give so-called nonlinear viscoelastic effects. Such considerations are implicit in the general nonlinear viscoelastic model, in which the time induced character is expressed by a memory function and the strain induced response by the dampening function. When, at fixed frequency and constant temperature, a pure, homogeneous polymer is submitted to an oscillatory strain of small amplitude, only time induced effects are observed and the viscoelastic behavior is linear; above a certain strain amplitude, strain induced effects bring a nonlinear response.

Pure, unfilled polymers essentially exhibit nonlinearity through the application of a sufficiently large strain and we call this behavior extra (or strain-induced) nonlinear viscoelasticity (because occurring through *external* causes, i.e., the applied strain). When polymer materials have a sufficient, sizeable level of heterogeneity, they are complex systems that exhibit morphology-induced effects, which superimpose to both time and strain induced effects. We call this behavior intra (or morphology-induced) nonlinear viscoelasticity (because owing to the *internal* morphology of the material). [Note that in previous reports<sup>4,5</sup> we used the adjectives intrinsic and extrinsic (instead of intra and extra); but such formal words may lead to misunderstanding of the views expressed above, owing to their usual meaning. For instance, intrinsic refers to qualities that are part of the basic nature or character of something. The above views concern the behavior of polymer systems, either with respect to their response to large amplitude strain or with respect to their morphology that further complicates their response. The adjectives "extra" and "intra" are therefore less ambiguous in the context.]

It is quite obvious that FT analysis of torque signal, while offering an attractive quantification of the nonlinear viscoelastic response, has limited capabilities to distinguish strain and morphology induced characters. Therefore FT analysis is supplemented by quarter cycle integration as an easy data treatment technique to distinguish extra and intra nonlinear viscoelasticity. The ratio of the first to second quarters torque signal integration, i.e.,  $Q1/Q2$  allows clearly distinguishing between the strain amplitude effect on a pure and a complex polymer materials. With the former,  $Q1/Q2$  ratio is always higher than

one and tends to increase with strain amplitude; in such a case the torque signal is always distorted "on the left" (i.e.,  $Q1 > Q2$ ). With certain complex systems,  $Q1/Q2$  is generally higher than one at (very) low strain, quickly passes below one with higher  $\gamma$ , then exhibits sometimes quite complex variations, for instance reaching a minimum value before going back asymptotically towards zero. Alternative methods have been proposed to quantify the distortion of the torque signal to the "left" or "right," for instance by considering the phases shift of the resulting harmonics.<sup>7,8</sup> Such methods, which require to have access to phase shift, are in their principle totally different and more complicated than our simple quarter cycle integration approach.

### Test materials

Two series of carbon black natural rubber masterbatches as described in Table I, were kindly supplied by Cabot Corp. (Boston, MA) as typical highly filled materials, with a near ideal dispersion state because prepared with a new patented technology, under trade name Cabot Elastomer Composites (CEC)<sup>TM</sup>. Series A has loadings from 35 to 75 phr, with a carbon black similar (but not equal) to N330; Series B ranges from 50 to 90 phr filler with a higher surface area but lower structure carbon black. CEC materials were received as friable lumps of loose small 5–8 mm strips, which were roughly molded at 100°C in 2–3 mm thick sheets. Owing to their very high stiffness at the standard testing temperature of 100°C, these samples were *a priori* considered as very challenging materials for advanced rheological testing. Indeed, as will be described below, a special sample handling procedure had to be adapted before reproducible and reliable results were obtained. According to Cabot, the supplied materials were prepared in Malaysia by the end of 2002, around 3 years before the experiments reported here were performed. Repeating some of our experiments by mid 2007 on samples stored at room temperature in darkness revealed no significant differences that could have been attributed to degradation effects.

CEC are produced at the company's facility in Port Dickson, Malaysia, through a patented continuous water phase mixing process for combining natural rubber latex and carbon black slurry. After dewatering and drying, resulting composites can be used in normal compounding operations, providing some unique rheological properties are taken into account in setting-up the mixing procedure. CECs are available in a number of standard grades, but can also be specially compounded to meet customers' individual requirements.<sup>9</sup> When compared with equivalent dry mixed masterbatches, CEC materials exhibit a higher and uniform level of dispersion, and after com-

TABLE I  
Test Materials; Cabot Elastomer Composites (CEC)<sup>TM</sup>

NR/Carbon black A series				NR/Carbon black B series			
Code name	Black content (phr)	$\Phi_{\text{Black}}$	Bound rubber* % ( $\pm 0.5$ )	Code name	Black content (phr)	$\Phi_{\text{Black}}$	Bound rubber* % ( $\pm 0.5$ )
NRA35	35	0.148	40.1	NRB50	50	0.199	55.9
NRA45	45	0.183	46.4	NRB60	60	0.230	60.2
NRA55	55	0.215	46.2	NRB65	65	0.244	61.3
NRA60	60	0.230	50.9	NRB70	70	0.258	62.7
NRA65	65	0.244	50.7	NRB75	75	0.271	69.0
NRA70	70	0.258	56.1	NRB80	80	0.284	77.8
NRA75	75	0.271	58.1	NRB90	90	0.309	78.1
Carbon black A				Carbon black B			
BET SA <sup>a</sup> (N <sub>2</sub> ), m <sup>2</sup> /g			111	BET SA <sup>a</sup> (N <sub>2</sub> ), m <sup>2</sup> /g			262
STSA <sup>b</sup> , m <sup>2</sup> /g			102	STSA <sup>b</sup> , m <sup>2</sup> /g			256
DBP <sup>c</sup> , mL/100 g			114.6	DBP <sup>c</sup> , mL/100 g			49.6
CDBP <sup>d</sup> , mL/100 g			94.0	CDBP <sup>d</sup> , mL/100 g			43.5

\* Measured in our laboratory by toluene extraction: 256 h. at room temperature.

<sup>a</sup> Supplier data; specific area through nitrogen adsorption, ASTM D-3037/4820 (ISO 4652).

<sup>b</sup> Supplier data; specific area through liquid nitrogen adsorption, ASTM D-4820/5816.

<sup>c</sup> Supplier data; structure through di-butyl phtalate absorption, ASTM D-2414 (ISO 4656).

<sup>d</sup> Supplier data; structure through di-butyl phtalate absorption after crushing, ASTM D-3493 (ISO 6894).

pounding and vulcanization have excellent physical properties, including higher tensile strength, lower hysteresis, and much longer flex life.<sup>10</sup> Because the dispersion process happens in the liquid phase, and the compound is subjected to minimum shearing forces during dewatering and drying, molecular weight preservation is claimed for elastomer composites, and therefore CEC materials of a given loading are expected to have a greatly higher polymer molecular weight than their equivalent dry mixes, while retaining the dispersion advantage. More intimate interactions occur between polymer and filler in CEC, as demonstrated by bound rubber values

which are typically 20–50% higher than for equivalent dry mixes. Improved hysteresis and flex fatigue life is attributed to the near “perfect” dispersion of carbon black/natural rubber composites.<sup>11,12</sup>

For the sake of comparison, a series of filled polybutadiene compounds, whose nonlinear viscoelastic properties had already been evaluated in the laboratory,<sup>13</sup> were added to the study (Table II). These samples were prepared in a 1.4-L Banbury mixer through an upside-down mixing procedure and sheeted off on open mill. Dump temperature was between 100 and 110°C and mixing energy in the 1550 mJ/m<sup>3</sup> range for all compounds, which were

TABLE II  
Test Materials; Polybutadiene Compounds

Compound coding	BR00B	BR10B	BR30B	BR50B	BR60B
High cis-1,4 BR <sup>a</sup>	100	100	100	100	100
N330 carbon black	–	10	30	50	60
Zinc oxide	5	5	5	5	5
Oil	5	5	5	5	5
Stearic acid	3	3	3	3	3
TMQ <sup>b</sup>	2	2	2	2	2
IPPD <sup>c</sup>	1	1	1	1	1
$\Phi_{\text{black}}$ <sup>d,e</sup>	0	0.043	0.119	0.184	0.213

<sup>a</sup> NeoCis BR40 (Polimeri); 98% cis-1,4; M<sub>w</sub> = 450.000 g/mol; MWD = 3.2.

<sup>b</sup> Tri-methyl quinoline, polymerized.

<sup>c</sup> Iso-propyl-paraphenylenediamine.

<sup>d</sup> Carbon black volume fraction.

<sup>e</sup> Specific gravity data used in calculation (g/cm<sup>3</sup>): BR 0.90; N330 1.80; ZnO 5.57; Oil 0.92; Stearic Acid 0.98; TMQ 1.08; IPPD 1.17.

stored at room temperature (23°C) under dark cover for several months before testing, to achieve all rubber-filler interactions.

## RESULTS AND DISCUSSION

### Experimental difficulties with highly filled rubber materials

After dump from internal mixer, high *cis*-1,4 polybutadiene compounds were cooled down and sheeted out on open mill, then compression molded at 100°C between polyester sheets into ~ 2.2 mm thick foils and allowed to cool down to room temperature under 5 kPa load. According to a well established practice, 46 mm diameter disks were die cut and compression molded (200 kPa) at 100°C, using a special mold with the same reciprocal cone geometry as the RPA but a 10% excess volume of the test cavity (0.125 radian cone–cone angle; volume: 3 cm<sup>3</sup>). No difficulties were met when testing the BR compounds using this test cavity loading procedure.

As previously demonstrated,<sup>14</sup> the RPA cavity must be fully loaded for reliable measurements and a slight volume excess of material is in fact needed, which contributes in the tight sealing of the test cavity. Indeed cavity filling experiments with either gum butadiene rubber or 50 phr N330 filled BR compounds have shown that reliable results are obtained when the loaded samples if between 110 and 160% of the cavity volume; the actual shape of the sample was not found relevant. When the RPA cavity is closing, radial flow occurs under axial compression and for most filled rubber compounds, the expected (central) gap (i.e., 0.485 mm with our instrument) is reached within 3–4 min. But, in addition to filler, common rubber compounds contain minor ingredients (in volume), i.e., stearic acid, oil, wax, which help the radial flow of the material in the cavity. CEC samples have very simple composition, just the elastomer matrix, the carbon black particles and minute quantities of antidegradant, and are consequently very stiff products, therefore far to correspond to typical rubber materials, even at temperature above 100°C. Unexpected experimental difficulties were met with such materials which prompted us to fix a linear displacement transducer to assess the actual test cavity closure during strain sweep tests (Fig. 3; right inset). The system was set such that a reading of 0.000 mm corresponds to perfect closure of the empty cavity. When testing various gum materials, gap closure of 0.008–0.100 mm were currently observed, so that it was concluded that 0.100 mm is in fact the ideal testing gap closure, which corresponds to a thin film of the same thickness compressed between the outer sealing rings of the cavity. Using 46 mm diameter disks cut out of a ~ 2 mm thick sheets made of loosely packed CEC

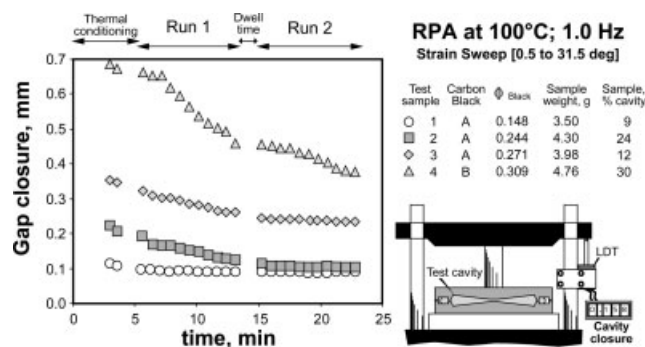


**Figure 3** Effect of sample volume and stiffness on gap closure during RPA strain sweep tests; test materials were CEC composites.

small strips, samples of known weight were used to perform strain sweep tests, while recording the variation of the gap closure.

As shown in Figure 3, only CEC composites with the lowest carbon black content achieve the ideal testing gap closure of around 0.100 mm, but it is the filler volume fraction (and hence the stiffness) of the material that is important rather than the loading volume of material. Indeed sample 3 (i.e., 0.271 carbon black fraction), while with a volume 12% in excess of the cavity never reached the ideal gap closure but achieved a constant closure of ~ 0.250 mm during run 2 of the strain sweep procedure. Sample 2 had a 24% volume excess but lower carbon black content and therefore reached the ideal gap closure. Sample 4 had both a large black content (and hence stiffness) and a large volume excess, and consequently was still far for the optimal gap closure after 23 min strain sweep test. We concluded from such experiments that, with stiff materials, not only the sample volume must be as close as possible to 110% of the empty cavity volume, but also that the actual shape of the sample was a relevant parameter. In consequence, all CEC samples were systematically prepared in the following manner: out of ~2 mm thick sheets made of loosely packed small strips, disks of 46 mm diameter were die cut and their weight adjusted to be close to the volume needed to load a mold with the same reciprocal cone geometry as the RPA but 10% volume excess. Compression molding between polyester films was made at 120°C under 200 kPa for 10 min, in such a manner that samples with volumes near the optimal 3.3 cm<sup>3</sup> and a similar geometry were used to load the RPA cavity. Only this tedious sample preparation procedure allowed obtaining reproducible results with the highly loaded CEC samples.

### Complex modulus versus strain amplitude

Figure 4 shows complex modulus versus strain curves for the polybutadiene compounds series, as

RPA-FT at 100°C ; 0.5 Hz; BR cpds

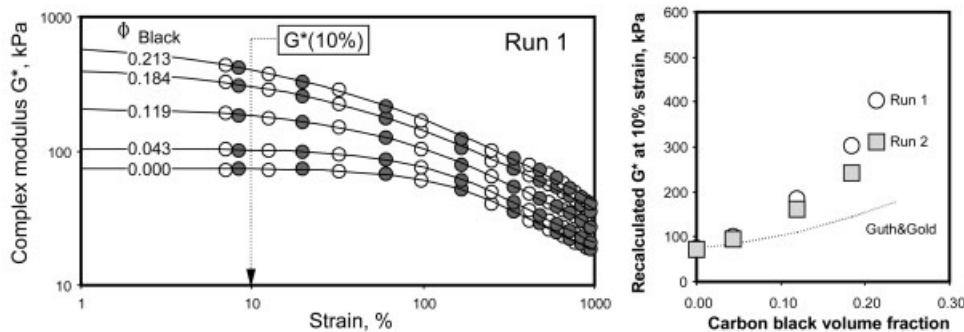


**Figure 4** Complex modulus versus strain amplitude curves for polybutadiene compounds;  $G^*$  at 10% strain as a function of filler volume fraction, in comparison with Guth and Gold model prediction [right graph].

measured at 0.5 Hz frequency. Similar curves are obtained with 1.0 Hz data but obviously slightly shifted vertically owing to the frequency effect. As can be seen, the end of the linear viscoelastic region is observable so long as the filler volume fraction remains below the so-called percolation level ( $\sim 0.12$ – $0.13$ ). Within the strain window of the RPA, no linear behavior can be observed for filler fraction above 0.119.

As previously reported,<sup>3–5</sup>  $G^*$  versus strain ( $\gamma_0$ ) curves are adequately modeled with the following simple equation:

$$G^*(\gamma_0) = G_f^* + \left[ \frac{G_0^* - G_f^*}{1 + (A\gamma_0)^B} \right] \quad (2)$$

where  $G_0^*$  is the modulus in the linear region,  $G_f^*$  the modulus for an infinite strain,  $A$  the reverse of a critical strain (which corresponds to  $(G_0^* - G_f^*)/2$ ), and  $B$  a parameter describing the strain sensitivity of the material. Table III gives fit parameters of eq. (2) for BR compounds tested at 0.5 and 1.0 Hz. [Note that  $1/A$  is given instead of  $A$ ]. It is worth noting that both  $G_0^*$  and  $G_f^*$  are extrapolated parameters, and therefore of limited meaning, if any, when their numerical value is too far from measured data. For instance, negative  $G_f^*$  values have no physical meaning and must therefore be discarded from any discussion. Fit parameters and eq. (2) allow to recalculate  $G^*$  values, within the experimental windows, for instance 10% strain, to compare samples with a de facto compensation for experimental scatter. As

**TABLE III**  
Filled Polybutadiene Compounds; Fit Parameters of Eq. (2)

G* vs. Strain: model parameters			Temp. (°C): 100				
Sample	$\Phi_{\text{Black}}$	Run (a&b)	$G_0^*$ (kPa)	$G_f^*$ (kPa)	1/A (%)	B	$r^2$
Freq. (Hz): 0.5							
BR00B	0.000	1	74.3	11.1	242.6	1.446	0.9994
		2	73.1	10.3	244.6	1.387	0.9994
BR10B	0.043	1	104.2	9.6	194.6	1.233	1.0000
		2	96.8	9.4	209.7	1.233	1.0000
BR30B	0.119	1	209.0	4.6	92.5	0.872	0.9999
		2	183.7	2.0	106.7	0.831	0.9999
BR50B	0.184	1	423.6	-3.2	37.9	0.695	0.9996
		2	338.9	-3.2	42.3	0.655	0.9998
BR60B	0.213	1	653.6	-9.0	21.7	0.648	1.0000
		2	519.5	-4.7	20.4	0.601	1.0000
Freq. (Hz): 1.0							
BR00B	0.000	1	103.0	18.1	208.7	1.545	0.9999
		2	102.6	17.0	211.9	1.510	0.9999
BR10B	0.043	1	139.7	15.8	171.3	1.309	1.0000
		2	131.9	14.7	188.3	1.321	1.0000
BR30B	0.119	1	263.8	9.7	88.0	0.939	0.9999
		2	227.2	10.0	109.4	0.952	1.0000
BR50B	0.184	1	464.8	10.2	48.0	0.840	0.9998
		2	362.5	14.4	58.8	0.821	0.9996
BR60B	0.213	1	721.4	6.9	27.8	0.781	0.9996
		2	478.7	26.2	36.9	0.800	0.9998



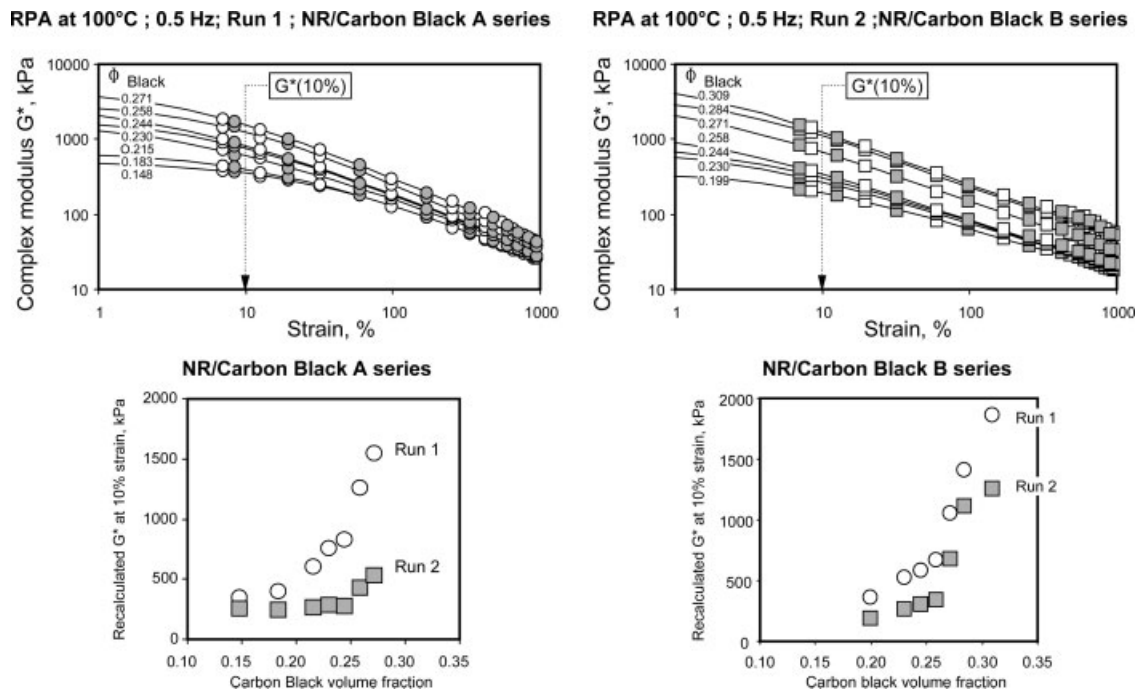


**Figure 5** Complex modulus versus strain amplitude curves for CEC series samples;  $G^*$  at 10% strain as a function of filler volume fraction.

shown in the right part of Figure 4, the linear modulus  $G_0^*$  increases strongly with the carbon black content, but expectedly in a manner markedly differing from the well known Guth-Gold-Simha model,<sup>15,16</sup> i.e.,  $G_{cpd} = G_0(1 + 2.5 \times \Phi_{black} + 14.1 \times \Phi_{black}^2)$ . The Guth-Gold-Simha equation is however based on mere hydrodynamic considerations and neither the complex structure of the filler, nor the rubber-filler interactions are taken into consideration. Another interesting aspect is the growing difference between runs 1 and 2, as carbon black fraction increases. The first strain sequence softens the material and the higher the filler level the larger the strain softening effect. The parameter  $A$  in eq. (2) is the reverse of a critical strain, and therefore  $1/A$  has the dimension of strain and is somewhat related with the extent of the linear viscoelastic region. The higher the filler level, the lower  $1/A$  with a significant strain history effect. Note that a finer assessment of the linear to nonlinear viscoelasticity transition would be obtained by considering the intersection between a horizontal line corresponding to  $G_0^*$  and a line passing through point  $[(G_0^* - G_f^*)/2, 1/A]$  and having a slope given by the first derivative of eq. (2) (see appendix). The strain sensitivity parameter  $B$  steadily decreases with  $\Phi_{black}$ .

Similar observations are made with the CEC series samples, as illustrated in Figure 5, with the corresponding fit parameters given in Tables IV and V. Such materials exhibit a strong nonlinear character and, consequently, recalculating  $G^*(10\%)$  offers a

safe manner to consider the carbon black fraction effect. As expected, the modulus strongly increases with carbon black content, so much so that it would practically impossible to process the highest loaded composites if they were not exhibiting a strong sensitivity to mixing or mastication, as indeed reported by the manufacturer.<sup>9,10</sup> Strain history effects are observed but samples prepared with carbon black B appear less sensitive (see lower graphs in Fig. 5). Such differences are likely related to carbon black size and structure, but in a complex manner since carbon black B has roughly twice the specific surface area of carbon A, while the latter absorbs twice more dibutyl phthalate than the former.

Parameters  $A$  and  $B$  of eq. (2) provide quite interesting information on the viscoelastic behavior of filled rubber compounds, with surprisingly relatively little effect of the matrix material, i.e., high *cis*-1,4 polybutadiene or natural rubber. As reported in Tables III–V, the critical strain  $1/A$  strongly decreases with higher carbon black fraction to be significantly below 50% when  $\Phi_{Black}$  is larger than 0.12 that is for all the CEC samples and the two highest loaded BR samples. This reinforces the comment made above that highly filled rubber compounds are essentially nonlinear materials.

Considering how the strain sensitivity parameter  $B$  varies with carbon black volume fraction, irrespective of the elastomer matrix, allows to make a very interesting observation (Fig. 6). As can be seen, the strain sensitivity decreases with increasing carbon



TABLE IV  
CEC/Carbon Black A; Fit Parameters of Eq. (2)

G* vs. Strain: model parameters			Temp. (°C): 100				
Sample	$\Phi_{\text{Black}}$	Run (a&b)	$G_0^*$ (kPa)	$G_f^*$ (kPa)	1/A (%)	B	$r^2$
Freq. (Hz): 0.5							
NRA35	0.148	1	507.3	(-0.8)	27.6	0.821	0.9999
		2	358.4	(-3.9)	33.1	0.730	0.9989
NRA45	0.183	1	677.1	1.6	15.9	0.788	0.9998
		2	486.3	(-3.7)	10.5	0.610	0.9999
NRA55	0.215	1	1845.0	(-6.5)	3.6	0.698	0.9971
		2	767.7	5.3	3.4	0.611	0.9958
NRA60	0.230	1	2012.0	(-1.6)	5.3	0.783	0.9999
		2	860.2	11.7	3.2	0.659	0.9965
NRA65	0.244	1	3058.0	(-7.1)	2.7	0.742	0.9997
		2	1235.0	13.7	1.4	0.641	0.9971
NRA70	0.258	1	2926.0	10.7	7.4	0.923	0.9979
		2	11,20.0	11.8	0.0	0.588	0.9995
NRA75	0.271	1	4779.0	1.4	4.2	0.850	0.9998
		2	3127.0	18.0	0.8	0.654	0.9990
Freq. (Hz): 1.0							
NRA35	0.148	1	591.6	(-4.7)	31.6	0.861	0.9995
		2	388.7	10.7	51.5	0.956	0.9977
NRA45	0.183	1	707.2	(-3.3)	24.2	0.849	0.9997
		2	422.1	6.3	35.4	0.821	0.9996
NRA55	0.215	1	1340.0	6.3	8.9	0.835	0.9997
		2	537.2	29.7	9.6	0.792	0.9977
NRA60	0.230	1	1940.0	6.2	5.9	0.819	0.9997
		2	609.0	38.4	9.0	0.837	0.9959
NRA65	0.244	1	2783.0	(-2.3)	3.9	0.790	0.9996
		2	977.0	33.5	3.2	0.721	0.9986
NRA70	0.258	1	4816.0	12.2	3.1	0.828	0.9997
		2	1859.0	45.7	2.1	0.712	0.9979
NRA75	0.271	1	4836.0	1.2	4.5	0.866	0.9995
		2	3308.0	31.1	0.7	0.630	0.9984

black content, but a minimum value appears to be reached when the filler volume fraction is around 0.20. This observation is made when materials are strained either at 0.5 or at 1.0 Hz frequency and we attribute the scatter at high  $\Phi_{\text{Black}}$  to difficulties in loading the RPA test cavity with very stiff materials, as discussed in the previous section.

### Relative harmonic components of torque signal

#### Experimental observations

At high strain amplitude, torque signals remain periodic but become distorted and FT resolves the measured signals in their components. Odd harmonics become significant as strain increases and are therefore considered as the nonlinear viscoelastic “signature” of the tested material. Figure 7 shows the typical pattern of both the corrected total torque harmonic content (TTHC), the 3rd and the 5th torque harmonic components, respectively,  $T(3/1)$  and  $T(5/1)$  versus strain  $\gamma$ , as exhibited by the polybutadiene compound without carbon black (BR00B) and the highest loaded BR sample (BR60B). As expected the TTHC curve envelopes the  $T(3/1)$  and the  $T(5/1)$  ones, and the 3rd harmonic bears the most signifi-

cant part of the information. As can be seen the unfilled material BR00B exhibits torque harmonics that evolve with strain amplitude in a smooth manner. One notes that 0.5 and 1.0 Hz data superimpose well with the former ones documenting a larger strain range than the latter. Minor ingredients in rubber formulations, for instance zinc oxide, stearic acid, oil, and chemicals, do not significantly affect the nonlinear viscoelastic response of the elastomer and therefore torque harmonics variations with strain amplitude are in qualitative agreement with similar observations on gum rubbers.<sup>17</sup> The 60 phr filled material shows a totally different behavior, with a “bump” appearing in the 500–600% strain range, essentially on the third relative harmonic (and of course on TTHC, total torque harmonic content). Similar curves are obtained with the other samples of the BR compounds series, and show that the size of the bump is increasing with higher carbon black content. One notes also a net strain history effect with the filled materials, in such a manner that run 2 curves exhibit a bump of slightly lower magnitude.

Figure 8 shows torque harmonic versus strain results obtained on the CEC samples, carbon black A series, run 1 data. Again no frequency effect is

TABLE V  
CEC/Carbon Black B; Fit Parameters of Eq. (2)

G* vs. Strain: model parameters			Temp. (°C): 100				
Sample	$\Phi_{\text{Black}}$	Run (a&b)	$G_0^*$ (kPa)	$G_f^*$ (kPa)	1/A (%)	B	$r^2$
Freq. (Hz): 0.5							
NRB50	0.199	1	736.2	1.2	9.6	0.778	0.9999
		2	388.6	8.0	9.4	0.739	0.9998
NRB60	0.230	1	1321.0	0.5	5.9	0.782	0.9999
		2	786.6	7.6	4.0	0.724	0.9998
NRB65	0.244	1	1317.0	4.3	7.6	0.840	0.9996
		2	910.1	9.7	3.9	0.756	0.9998
NRB70	0.258	1	1428.0	6.1	8.7	0.885	1.0000
		2	1410.0	10.4	2.2	0.749	0.9998
NRB75	0.271	1	2607.0	14.7	6.4	0.908	0.9999
		2	3687.0	11.2	1.4	0.752	0.9998
NRB80	0.284	1	2891.0	31.8	9.3	0.996	0.9999
		2	3864.0	35.2	3.4	0.857	1.0000
NRB90	0.309	1	5498.0	27.0	4.8	0.923	0.9984
		2	6883.0	33.3	1.6	0.820	0.9995
Freq. (Hz): 1.0							
NRB50	0.199	1	767.5	8.6	11.4	0.845	0.9997
		2	391.2	22.2	13.0	0.845	0.9994
NRB60	0.230	1	1258.0	10.3	8.3	0.872	0.9999
		2	705.3	23.5	6.4	0.801	0.9998
NRB65	0.244	1	1466.0	10.1	7.2	0.865	0.9998
		2	753.6	27.7	6.2	0.837	0.9999
NRB70	0.258	1	1774.0	9.7	7.2	0.891	0.9993
		2	1242.0	27.3	3.1	0.797	0.9994
NRB75	0.271	1	2980.0	9.4	5.6	0.892	0.9986
		2	1589.0	41.9	5.4	0.899	0.9994
NRB80	0.284	1	3327.0	28.9	8.3	0.991	0.9995
		2	3612.0	43.2	2.8	0.822	0.9997
NRB90	0.309	1	4339.0	53.6	8.0	1.050	0.9997
		2	6708.0	65.8	1.5	0.836	0.9995

observed since 0.5 and 1.0 Hz data superimpose well. Similar data are obtained on the carbon black B series. In terms in filler volume fraction, the highest loaded BR samples overlap the lowest loaded CEC samples and observations made on the former are complemented by results on CEC materials. Above a sufficient filler loading, presumably the so-called percolation level 0.12–0.13, torque harmonics versus strain amplitude curves exhibit a local maximum, or

“bump,” whose magnitude and maybe position (on the strain scale) change with the filler content. Such results suggest that filler particles enhance the non-linear response of the rubber matrix but that this additional nonlinearity tends to disappear as the strain amplitude is becoming larger. One clearly needs strain sweep tests at 0.5 Hz to detect such effects, owing to the limited strain range at higher frequency.

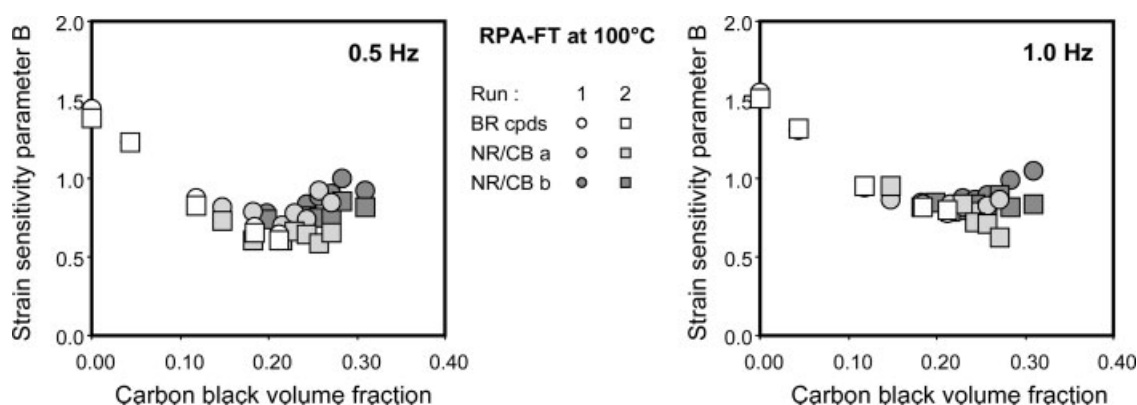
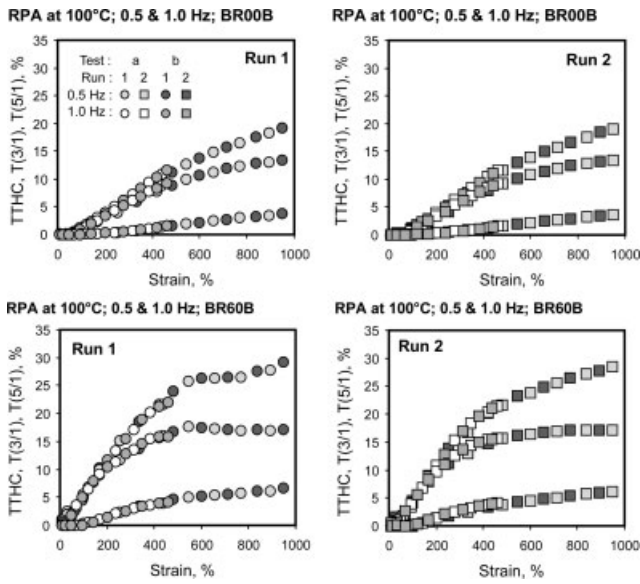


Figure 6 Strain sensitivity parameter B versus carbon black volume fraction; all samples investigated.



**Figure 7** Typical torque harmonic responses for high *cis*-1,4 polybutadiene compounds; strain sweep tests at 0.5 and 1.0 Hz; BR00B contains no carbon black, only the usual compounding ingredients; BR60B is the 60 phr N300 black content sample.

Developing a model for torque harmonics variation with strain amplitude

Odd torque harmonics become significant as strain increases and are therefore considered as the nonlinear viscoelastic “signature” of tested materials, only available through FT rheometry. Numerous RPA-FT experiments on various pure, unfilled polymers have shown that relative torque harmonics vary with

strain amplitude in such a manner that an initial S-shape curve appears bounded by a simple linear variation at high strain. Accordingly, the following equation was successfully used in treating results obtained on a series of gum natural rubbers<sup>17</sup>:

$$TH(\gamma) = (TH_m + \alpha\gamma_0) \times [1 - \exp(-C\gamma_0)]^D \quad (3)$$

where  $\gamma_0$  is the strain magnitude,  $TH_m$ ,  $\alpha$ ,  $C$ , and  $D$  parameters of the model. The member  $(TH_m + \alpha\gamma_0)$  expresses a linear variation of harmonics in the high strain region, while the member  $[1 - \exp(-C\gamma_0)]^D$  describes the development of the nonlinear viscoelastic response. The physical meaning of parameters  $TH_m$  and  $\alpha$  is obvious; parameter  $D$  somewhat reflects the extend of the linear viscoelastic region (i.e., where no harmonics are detected), while parameter  $C$  indicates the strain sensitivity of the nonlinear character. Equation (3) corresponds to asymptotically zero harmonics, as the strain  $\gamma$  is smaller and smaller, in other words in the linear viscoelastic region, in complete agreement with theory.

Results obtained on sufficiently filled rubber compounds do not correspond to the simple behavior expressed by eq. (3), since a “bump” is observed in the intermediate strain region, while at high strain, either TTHC or  $T(3/1)$  versus strain curves remain asymptotic to a simple linear variation. It is worth noting that such results are obtained on systems in which strong interactions occur between a viscoelastic matrix (i.e., the major volume phase) and a dispersed phase (i.e., the carbon black). Therefore, one could draw the hypothesis that this typical variation

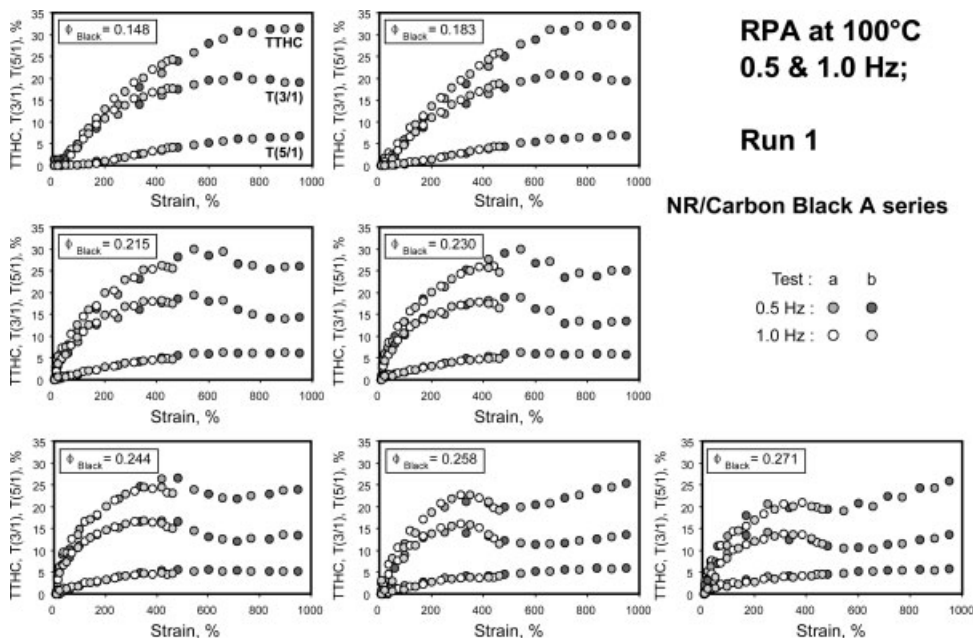


**Figure 8** Typical torque harmonic responses for CEC samples, carbon black A series; strain sweep experiments at 0.5 and 1.0 Hz; run 1 data.

reflects the superimposition of two responses (or curves): one qualitatively common to all “pure” (or virgin, unfilled) polymers and readily well modeled by eq. (3), and a curve that would pass through a maximum at a typical strain value and would express the “filler response.” What would be the physical reasoning in selecting the most appropriate mathematical model for the filler response? In other terms, why do filled rubber compounds exhibit a singularity in harmonics at a typical strain amplitude? There are at least two elements for a possible answer: (1) interactions between phases enrich the harmonic response of the system at the onset of the nonlinear region; (2) above a critical strain, such interactions start to be destroyed (or at least modified) and their effects vanish at sufficiently large strain amplitude.

With such considerations in mind, the source of an appropriate mathematical handling of the filler response was sought in the manner failure modes in industrial operations are currently analyzed. For instance, the so-called Weibull analysis\* has been proved to be very useful in matching historical failure and repair data to appropriate probability density functions which represent the characteristics of a given failure mode in the course of any (complex) industrial process. The three parameters Weibull probability density function is given by

$$f(x) = \frac{\alpha}{\beta} \left( \frac{x - \gamma}{\beta} \right)^{\alpha-1} \exp \left[ - \left( \frac{x - \gamma}{\beta} \right)^\alpha \right]$$

where  $f(x) \geq 0$ ,  $x \geq 0$  or  $\gamma, \beta > 0$ ,  $-\infty < \gamma < +\infty$ ;  $\beta$  is the so-called scale parameter,  $\gamma$  the shape parameter, and  $\alpha$  the location parameter. The shape parameter  $\alpha$  is particularly interesting in the present context because it is a dimensionless number whose value affects the form of the distribution; particularly when  $\alpha$  is in the range 2.5–3.7, “bell shape” distribution curves are obtained.

The logics behind the Weibull analysis can consequently be transposed to the torque harmonics variation with strain magnitude of filled systems by considering that, because of strong interactions between the viscoelastic matrix and the discrete phase, a kind of soft composite network is embedded in the (free) rubber phase. The soft composite would consist of the carbon black particles in interaction with the bound rubber. It follows that there are initially additional harmonics in the medium strain range, which enhance the ongoing nonlinear response of the matrix, then as strain further increases, filler-polymer interactions decrease and eventually vanish in such

a manner that, for sufficiently high strain amplitude, essentially the high strain response of the polymer plays yet a role. A model was consequently developed to add Weibull considerations to the behavior expressed by eq. (3), while keeping a minimum number of parameters, for the sake of simplicity. After various attempts, a simple five parameters equation was eventually derived:

$$\text{TH}(\gamma_0) = (\text{TH}_m + \alpha\gamma_0) \times \{ [1 - \exp(-\alpha\gamma_0)]^{\text{TH}_m} + B(C\gamma_0)^{D-1} \exp[-(C\gamma_0)^D] \} \quad (4)$$

where  $\text{TH}(\gamma_0)$  stands for any relative torque harmonic, i.e.  $T(n\omega/1\omega)$ , and also for the so-called total torque harmonic content TTHC [i.e.  $\sum T(n\omega/1\omega)$ ]. With respect to the nonlinear fitting of this equation to experimental results, it was quite significant to find that the S-shape polymer response could be modeled with only two parameters,  $\text{TH}_m$  and  $\alpha$ , instead of four as in eq. (3). The physical meaning of the parameters of eq. (4) can be understood when considering the mathematical virtues of the model. In fact, eq. (4) consists of three members:

one describing the asymptotic high strain behavior:

$$(\text{TH}_m + \alpha\gamma_0) \quad (4a)$$

one describing the polymer response, the so-called polymer component:

$$(\text{TH}_m + \alpha\gamma_0) \times (1 - \exp(-\alpha\gamma_0))^{\text{TH}_m} \quad (4b)$$

one describing the filler response, the so-called filler component:

$$(\text{TH}_m + \alpha\gamma_0) \times B(C\gamma_0)^{D-1} \exp(-[(C\gamma_0)^D]) \quad (4c)$$

As illustrated in Figure 9, drawing curves with eq. (4a,b) and typical experimental parameters reveals some interesting aspects of the model.

As can be seen the actual torque harmonics variation with strain amplitude of filled polymer material consists of a smooth polymer response to which a filler response is added in the medium strain range. At low strain, the nonlinear character is essentially controlled by the filler component, i.e., the  $(\text{TH}_m + \alpha\gamma_0) \times B(C\gamma_0)^{D-1} \exp(-[(C\gamma_0)^D])$  term. At higher strain, the influence of the filler vanishes and harmonics variation is essentially controlled by the polymer component. The maximum of the filler component curve corresponds to a critical strain, i.e.,  $\gamma_{c2}$ , at which decreasing polymer-filler interaction would start to override the nonlinear character enhancement due to the dispersed phase. The actual maximum in the measured torque harmonics corresponds to the critical strain  $\gamma_c$ , obviously higher than  $\gamma_{c2}$  owing to the high strain asymptote member. At suf-

\*Named after the Swedish engineer Waloddi Weibull (1887–1979) who used a special family of distribution functions for reliability analysis in metallurgical failure modes.



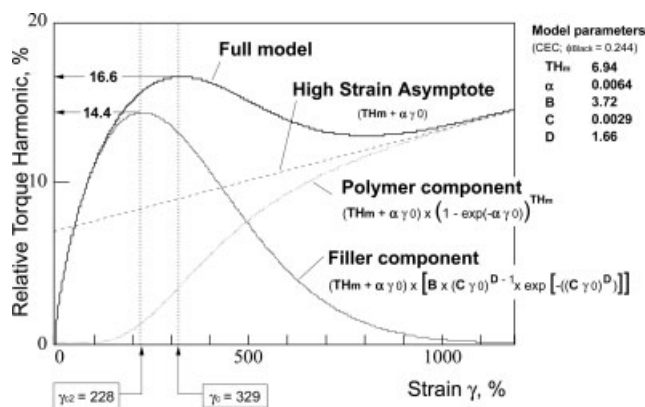


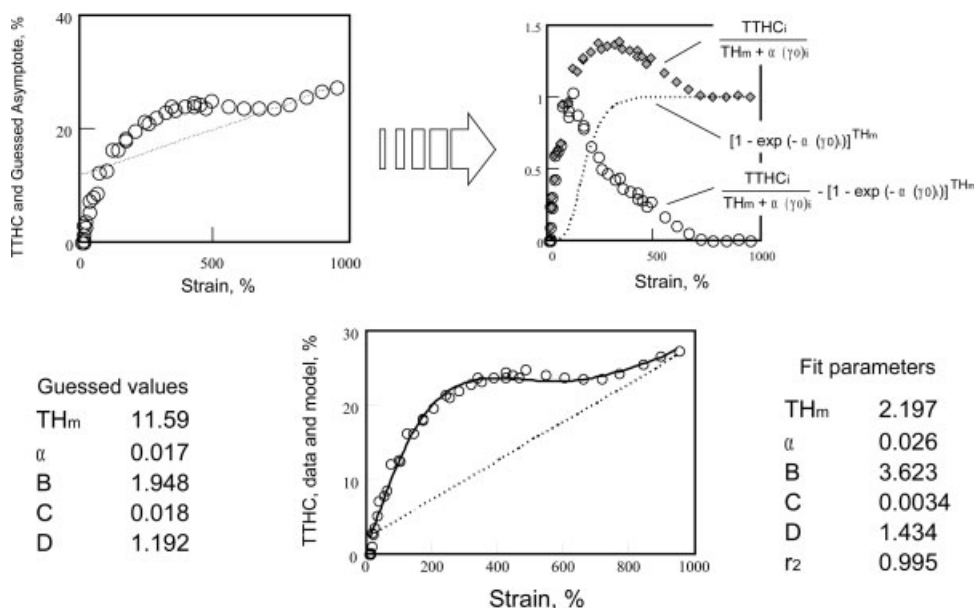
**Figure 9** Mathematical virtues of the model for relative torque harmonics variation with strain amplitude; note that curves were calculated with fit parameters of actual experimental results.

ficiently high strain, the effect of the filler is reduced to mere hydrodynamic influences. One expects of course the parameter  $B$  to increase with higher filler content and to be zero for a pure polymer, in which case eq. (4) reduces to eq. 4(b). As soon as the model parameters have been determined by fitting eq. (4) to experimental data (using for instance a nonlinear regression algorithm of the Marquard-Levenberg type) easy mathematical handling yields the critical strains, as well as any remarkable features such as the maximum of the “bump.”

**Nonlinear fitting of experimental torque harmonics versus strain data**

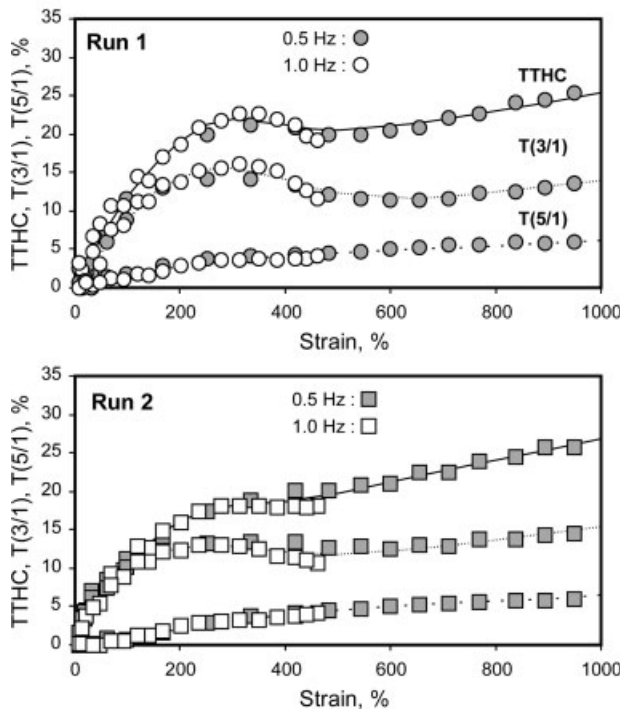
A standard technique for nonlinear least-squares fitting problems in a large spectrum of disciplines is

nowadays the Levenberg-Marquardt (LM) algorithm, readily available in many commercial calculation software. Essentially the LM algorithm is an iterative procedure that locates the minimum of a multivariate function, which is expressed as the sum of squares of nonlinear real-valued function. We used the LM algorithm implemented in Mathcad 8.0 (MathSoft Inc., Cambridge, MA) which requires partial derivatives of the model with respect to all parameters and initial “guessed values” for the parameters. For a five parameters model [eq. (4)], the goodness of the fit is extremely sensitive to the initial guesses, but the mathematical virtues of the model allow adequate initial data to be extracted through easy handling of the experimental data set. For all tested materials in the present study, no significant effect of frequency was observed on relative torque harmonics, and therefore a full data set consisted of the merging of the relative torque harmonics, i.e.,  $TH_i$ , essentially either TTHC,  $T(3/1)$  or  $T(5/1)$ , as measured versus strain amplitude  $(\gamma_0)_i$  on two samples (A and B), at 0.5 and 1.0 Hz frequency. After sorting the data set (i.e.,  $2 \times 20 = 40$  data points per run) by increasing strain amplitude, fair estimates of  $TH_m$  and  $\alpha$  are immediately obtained through linear regression of the last 3–7 points. Then the high strain asymptotic behavior is “neutralized” by dividing all data  $TH_i$  by  $(TH_0 + \alpha(\gamma_0)_i)$ . The guessed component  $[1 - \exp(-\alpha(\gamma_0)_i)]^{TH_m}$  is then calculated and subtracted from the previous results to yield data points along an asymmetrical bell shape curve which corresponds to the filler component. The guessed value for  $B$  is taken as the maximum of the filler component and a fair estimate for  $D$  is obtained by considering that before the maxi-



**Figure 10** Strategy for nonlinear fitting of eq. (4) to experimental torque harmonics versus strain data.

## RPA at 100°C; 0.5 &amp; 1.0 Hz; tests a &amp; b

NR/Carbon Black A :  $\phi_{\text{Black}} = 0.258$ 

**Figure 11** Modeling torque harmonics versus strain variation; strain sweep tests (100°C; 0.5 and 1.0 Hz) on CEC/70 phr carbon black A.

imum, the term  $(C\gamma)^{D-1}$  is preponderant. Eventually, the guessed value for  $C$  is calculated from the first data points. Figure 10 illustrates this procedure. The

guessed parameters  $TH_m$ ,  $\alpha$ ,  $B$ ,  $C$ , and  $D$  so obtained are used to run the Levenberg-Marquardt algorithm. As shown in the Figure, the nonlinear algorithm yields fit parameters which may be substantially different from the initial estimates provided by the procedure described above, but nevertheless provide an elegant manner to abstract a large quantity of experimental data in only five parameters with a precise physical meaning.

## Effect of filler loading on torque harmonics versus strain model parameters

Figures 11 and 12 illustrate how the eq. (4) model suits experimental data. Despite the experimental scatter, likely due to difficulties in meeting the ideal sample volume/shape as discussed above (Experimental difficulties with highly filled rubber materials Section), fits are generally excellent and could be better if data gathered at 0.5 Hz only were used. Such figures demonstrate that one can discuss results in confidence by considering model parameters only.

Model parameters obtained when fitting experimental results with eq. (4) are given in Tables VI–VIII for all the investigated materials, as well as critical strain values that are easily calculated using the parameters and single recursive algorithms. As illustrated in Figure 9, the critical strain  $\gamma_c$  is the position (on the strain scale) of the “bump” observed on experimental data, while the critical strain  $\gamma_{c2}$  gives the position of the maximum value of the filler component [eq. (4c)]. The strain  $\gamma_m$  is the deformation at

## RPA at 100°C; 0.5 &amp; 1.0 Hz; tests a &amp; b

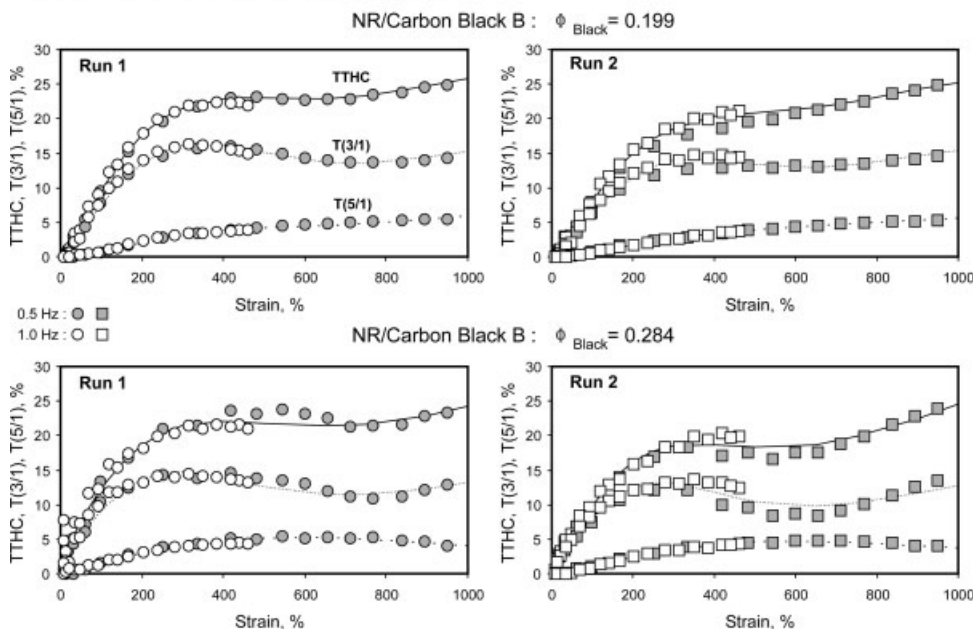


**Figure 12** Modeling the variation of torque harmonics versus strain; strain sweep tests (100°C; 0.5 and 1.0 Hz); CEC/carbon black B samples (50 and 80 phr).

TABLE VI  
High *cis*-1,4 Polybutadiene/N330 Compounds; Model Parameters for Total Torque Harmonics Content and Relative 3rd Torque Harmonic vs. Strain Amplitude; Strain Sweep Tests at 100°C, 0.5 and 1.0 Hz Frequency

$\Phi_{\text{Black}}$ :	0.000		0.043		0.119		0.184		0.213	
	TTHC		TTHC		TTHC		TTHC		TTHC	
	Run 1	Run 2	Run 1	Run 2	Run 1	Run 2	Run 1	Run 2	Run 1	Run 2
$\text{TH}_m$	14.49	4.01	3.87	4.60	4.48	6.07	4.69	6.49	3.29	6.12
$\alpha$	0.0059	0.0082	0.0090	0.0096	0.0125	0.0126	0.0209	0.0153	0.0241	0.0161
$B$	0.88	1.47	1.59	1.21	1.33	0.69	1.06	0.94	1.46	1.29
$C$	0.0025	0.0009	0.0009	0.0009	0.0012	0.0011	0.0017	0.0014	0.0019	0.0014
$D$	2.64	1.99	2.04	2.12	2.13	1.93	2.60	1.97	2.05	1.80
$r^2$	0.9993	0.9996	1.0000	1.0000	0.9992	0.9988	0.9996	0.9992	0.9987	0.9993
$\gamma_c$	343	1016	1029	1029	773	813	563	636	499	627
$\gamma_{c2}$	428	122	97	84	65	83	10	82	20	101
$\gamma_m$	1149	4610	4492	4237	3161	3893	1749	2997	2113	3461
	T(3/1)		T(3/1)		T(3/1)		T(3/1)		T(3/1)	
	Run 1	Run 2	Run 1	Run 2	Run 1	Run 2	Run 1	Run 2	Run 1	Run 2
$\text{TH}_m$	4.71	4.79	3.50	3.89	3.04	3.87	13.06	15.75	12.97	15.50
$\alpha$	0.0098	0.0098	0.0091	0.0092	0.0119	0.0116	0.0047	0.0045	0.0051	0.0046
$B$	0.00	0.02	0.73	0.59	1.09	0.78	2.01	1.78	2.11	1.93
$C$	0.1571	0.2460	0.0014	0.0015	0.0018	0.0020	0.0019	0.0020	0.0021	0.0020
$D$	17.97	1.73	2.36	2.33	2.34	2.39	2.19	2.36	2.06	2.20
$r^2$	0.9982	0.9985	0.9990	1.0000	0.9994	0.9987	0.9978	0.9982	0.9981	0.9986
$\gamma_c$	n/a	n/a	665	614	521	461	417	409	365	394
$\gamma_{c2}$	n/a	n/a	n/a	n/a	n/a	n/a	343	n/a	321	373
$\gamma_m$	n/a	n/a	n/a	n/a	n/a	n/a	1915	n/a	1871	1807

(n/a = non available).

which all filler effects have vanished, in other terms when the model parameter curve merges with the S-shape curve corresponding to the polymer component [eq. (4b)]. Since both curves merge asymptotically,  $\gamma_m$  is readily calculated through a recursive routine that locates the strain at which the overall model curve and eq. (4b) are within 0.001 unit (i.e., %) each other. It is fairly obvious that eq. (4) is not expected to correspond well to the nonlinear behavior of unfilled or not sufficiently filled materials. Consequently, parameters  $B$ ,  $C$ , and  $D$ , which are given only for consistency, have no physical meaning for the unfilled and the low filled BR compounds; therefore no critical strain values are obtained.

Parameters given in Table VI–VIII allow to perform a very fine analysis of the nonlinear viscoelastic behavior of (uncured) filled rubber compounds and, at first glance, reveal a number of interesting features. With respect to our approach in developing the model, parameters  $\text{TH}_m$  and  $\alpha$  describe in principle the asymptotic nonlinear behavior at infinite strain, i.e., when all rubber-filler interactions have expectedly be destroyed and when the viscoelastic character is maintained only by the stretched rubber phase. One would therefore expect  $\text{TH}_m$  and  $\alpha$  to be the same for a given type of formulation, irrespective

of the filler content. This is not the case as, generally, the  $\text{TH}_m$  parameter decreases with increasing filler content, while parameter  $\alpha$  tends to increase. However, the available experimental window is limited to some 1000% strain, which is obviously not large enough to ensure a full destruction of all filler-interactions. Since the accuracy of fit parameters is related to the size of the experimental window, observed variations of  $\text{TH}_m$  and  $\alpha$  with carbon black fraction could be artifacts. Conversely, one could also argue that such variations reflect a kind of strain amplification effect since the higher the filler fraction, the larger the strain supported by the polymer matrix.

As shown in Figure 13, the parameter  $B$  increases with the filler content and, expectedly tends to vanish for low filled or unfilled compounds, in agreement with the development of the model. One notes also that no strain history effect seems appearing on  $B$  (no differences between run 1 and 2) and that the level of carbon black rather than its structure is the key factor. Since  $B$  is concerned with the nonlinear modeling of carbon black effects, the nature of the rubber matrix (here natural rubber or polybutadiene) plays no role.

Torque harmonics associated with the response of filled rubber compounds to large amplitude oscilla-

TABLE VII  
 CEC Samples; Carbon Black A Series; Model Parameters for Total Torque Harmonics Content and Relative 3rd Torque Harmonic vs. Strain Amplitude; Strain Sweep Tests at 100°C, 0.5 and 1.0 Hz Frequency

$\Phi_{\text{black}}$	0.148		0.183		0.215		0.230		0.244		0.258		0.271	
	Run 1	Run 2	Run 1	Run 2	Run 1	Run 2	Run 1	Run 2	Run 1	Run 2	Run 1	Run 2	Run 1	Run 2
$TH_m$	27.63	7.26	20.06	6.72	16.98	17.28	16.22	15.10	14.81	13.21	14.02	13.07	13.54	12.83
$\alpha$	0.0055	0.0170	0.0042	0.0146	0.0067	0.0090	0.0076	0.0102	0.0095	0.0110	0.0113	0.0137	0.0120	0.0135
$B$	1.69	1.02	2.63	1.69	2.44	1.76	2.48	1.82	2.44	1.94	2.26	1.74	2.11	1.85
$C$	0.0018	0.0013	0.0014	0.0014	0.0022	0.0032	0.0025	0.0035	0.0032	0.0038	0.0040	0.0053	0.0045	0.0053
$D$	2.26	1.77	2.05	1.81	1.76	2.17	1.73	1.99	1.72	1.85	1.98	1.84	1.80	1.80
$r^2$	0.9985	0.9964	0.9983	0.9967	0.9955	0.9958	0.9927	0.9932	0.9910	0.9940	0.9934	0.9955	0.9922	0.9942
$\gamma_c$	441	668	539	615	305	245	263	214	206	265	187	133	153	130
$\gamma_{c2}$	661	95	914	150	562	366	495	324	385	376	303	221	272	226
$\gamma_m$	1959	3829	2876	3463	2275	1150	2063	1178	1622	2408	1044	868	1061	902
	T(3/1)		T(3/1)		T(3/1)		T(3/1)		T(3/1)		T(3/1)		T(3/1)	
$TH_m$	16.15	16.91	14.95	16.52	7.65	10.33	6.81	8.66	6.94	10.89	7.64	7.55	12.70	7.00
$\alpha$	0.0047	0.0049	0.0045	0.0046	0.0042	0.0056	0.0049	0.0063	0.0064	0.0048	0.0065	0.0079	0.0042	0.0077
$B$	2.06	1.89	2.25	2.06	3.96	2.69	4.21	2.96	3.72	2.54	3.54	2.81	2.21	3.07
$C$	0.0019	0.0021	0.0018	0.0020	0.0020	0.0026	0.0023	0.0030	0.0029	0.0026	0.0033	0.0040	0.0025	0.0040
$D$	2.15	2.33	2.08	2.36	1.72	2.04	1.67	1.95	1.66	1.79	1.98	1.74	1.80	1.70
$r^2$	0.9963	0.9950	0.9980	0.9956	0.9933	0.9955	0.9906	0.9950	0.9880	0.9920	0.9873	0.9868	0.9843	0.9892
$\gamma_c$	409	387	425	408	338	294	288	267	228	260	230	171	269	167
$\gamma_{c2}$	375	359	387	384	386	284	329	230	245	338	239	185	383	190
$\gamma_m$	1971	1603	2169	1665	2593	1535	2381	2555	1884	1856	1265	1252	1905	1304



TABLE VIII  
 CEC Samples; Carbon Black B Series; Model Parameters for Total Torque Harmonics Content and Relative 3rd Torque Harmonic vs. Strain Amplitude; Strain Sweep Tests at 100°C, 0.5 and 1.0 Hz Frequency

φblack:	0.199		0.230		0.244		0.258		0.271		0.284		0.309	
	TTHC		TTHC		TTHC		TTHC		TTHC		TTHC		TTHC	
	Run 1	Run 2	Run 1	Run 2	Run 1	Run 2	Run 1	Run 2	Run 1	Run 2	Run 1	Run 2	Run 1	Run 2
TH <sub>m</sub>	19.30	17.72	16.96	16.68	2.16	2.48	2.11	15.24	2.21	2.21	1.88	1.36	9.16	1.18
α	0.0069	0.0077	0.0082	0.0086	0.0240	0.0244	0.0250	0.0106	0.0259	0.0274	0.0210	0.0230	0.0105	0.0218
B	2.23	1.93	2.41	2.04	4.01	2.87	4.19	2.14	3.61	3.00	4.23	3.77	2.72	4.80
C	0.0027	0.0030	0.0031	0.0034	0.0033	0.0034	0.0037	0.0042	0.0034	0.0035	0.0032	0.0037	0.0035	0.0041
D	2.12	2.17	2.05	2.10	1.55	1.55	1.51	1.94	1.44	1.42	1.33	1.48	1.55	1.48
r <sup>2</sup>	0.9991	0.9979	0.9989	0.9981	0.9978	0.9977	0.9971	0.9973	0.9951	0.9966	0.9846	0.9927	0.8644	0.9890
γ <sub>c</sub>	285	260	244	226	247	212	238	173	235	190	267	246	174	222
γ <sub>c2</sub>	487	419	419	374	478	381	367	304	507	338	435	347	347	356
γ <sub>m</sub>	1415	1233	1295	1134	1279	1118	1825	1023	1470	1097	2725	1881	1758	1693
	T(3/1)		T(3/1)		T(3/1)		T(3/1)		T(3/1)		T(3/1)		T(3/1)	
	Run 1	Run 2	Run 1	Run 2	Run 1	Run 2	Run 1	Run 2	Run 1	Run 2	Run 1	Run 2	Run 1	Run 2
TH <sub>m</sub>	10.86	10.26	9.55	9.98	9.26	9.56	9.63	9.32	1.41	1.52	1.33	1.27	1.09	2.15
α	0.0052	0.0057	0.0053	0.0057	0.0054	0.0059	0.0056	0.0064	0.0135	0.0154	0.0117	0.0115	0.0082	0.0076
B	2.89	2.51	3.35	2.75	3.49	2.91	3.31	2.95	5.67	4.91	6.18	5.94	8.70	6.51
C	0.0026	0.0028	0.0027	0.0029	0.0028	0.0030	0.0031	0.0033	0.0036	0.0039	0.0036	0.0039	0.0038	0.0036
D	2.04	2.09	1.98	2.01	1.96	1.97	1.94	1.88	1.53	1.51	1.46	1.60	1.44	1.69
r <sup>2</sup>	0.9972	0.9955	0.9977	0.9963	0.9968	0.9967	0.9975	0.9958	0.9911	0.9929	0.9789	0.9791	0.8839	0.9749
γ <sub>c</sub>	292	276	277	260	247	223	236	218	250	191	234	222	212	218
γ <sub>c2</sub>	315	274	307	277	478	381	288	245	507	338	183	175	279	238
γ <sub>m</sub>	1541	1378	1553	1410	1279	1118	1386	1357	1470	1097	1959	1523	1924	1496

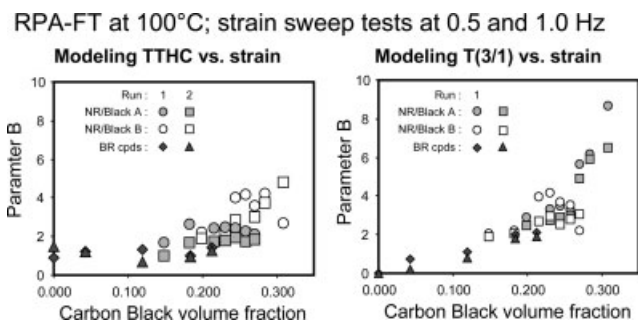


**Figure 13** Studying nonlinear effects of carbon black through torque harmonics versus strain data, as model with eq. (4); effect of filler fraction on parameter B; all samples tested.

tory strain reveal thus that, in addition to the nonlinear response of the rubber matrix, there is an enhanced nonlinearity due to filler particles, quantitatively well assessed through the parameters of eq. (4) (Figs. 14 and 15). In developing the model (Developing a model for torque harmonics variation with strain amplitude, Section), it was explicitly considered that filler particles are enhancing the viscoelastic response of the material in such a manner that above a certain strain, there is a reversal of the effect until it completely vanishes at very high strain amplitude. One may note here that such views are in agreement with the “filler network” concept used to explain well known reinforcement phenomena, for instance the so-called Payne effect,<sup>18</sup> or more recent considerations such as the fractal cluster-cluster aggregation model proposed by Klüppel and Heinrich.<sup>19,20</sup> Easy mathematical handling of eq. (4), using the model parameters given in Table VI–VIII allows to determine the critical strain at which the maximum nonlinear effect of the filler is obtained. Calculation are of course more precise if one considers the third relative torque harmonic  $T(3/1)$ . As

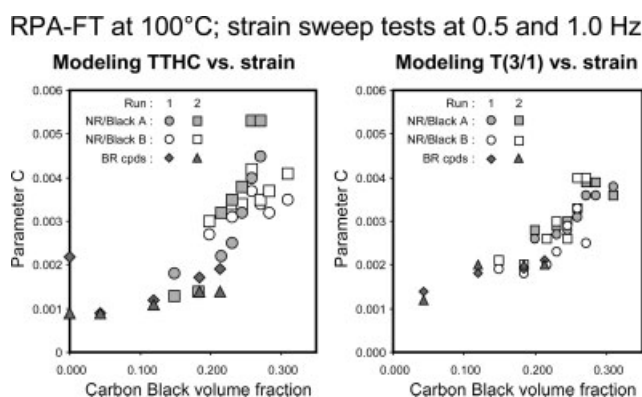


**Figure 14** Studying nonlinear effects of carbon black through torque harmonics versus strain data, as model with eq. (4); effect of filler fraction on parameter C; all samples tested.

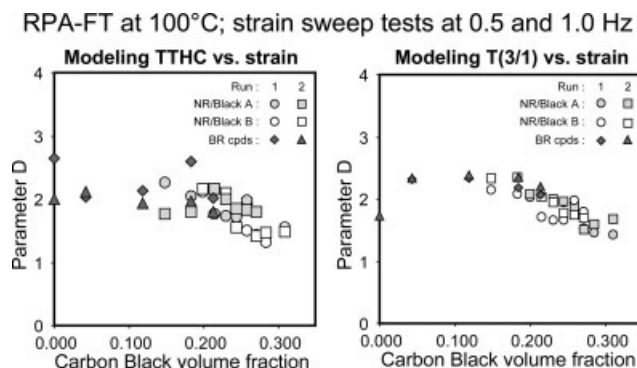


**Figure 15** Studying nonlinear effects of carbon black through torque harmonics versus strain data, as model with eq. (4); effect of filler fraction on parameter D; all samples tested.

shown in Figure 16, the critical strain decreases with increasing carbon black content, irrespective of the polymer, high *cis*-1,4 BR or natural rubber, with very little, if any, effect of the carbon black type. The highest filler content of the series of investigated materials is 90 phr (or 0.309 volume fraction), likely a maximum level with respect to most industrial applications; it can therefore be claimed that the materials considered in this study are covering the full range of (carbon black) filled rubber compounds. Consequently, Figure 16 is offering a very elegant demonstration of the essential nonlinear viscoelastic character of all practical rubber formulations and moreover reinforces the implicitly nonlinear nature of such materials, otherwise readily appearing through the quarter cycle integration method discussed in the next section.

### Quarter cycle integration

By integrating the two first quarters of the (averaged) torque signal resulting from the application of

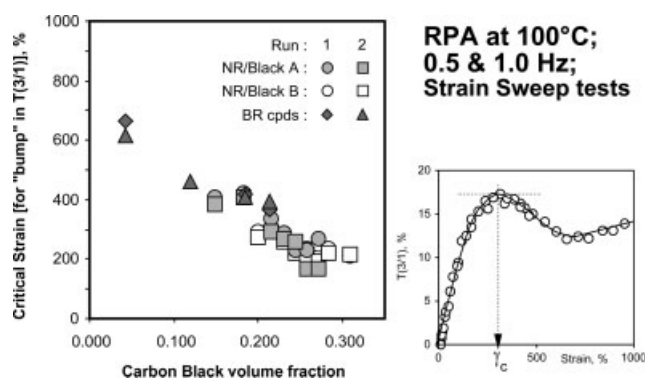


**Figure 16** Critical strain for maximum nonlinear viscoelastic effects owing to carbon black; derived through mathematical handling of eq. (4) with model parameters given in Tables VI to VIII; all samples tested.

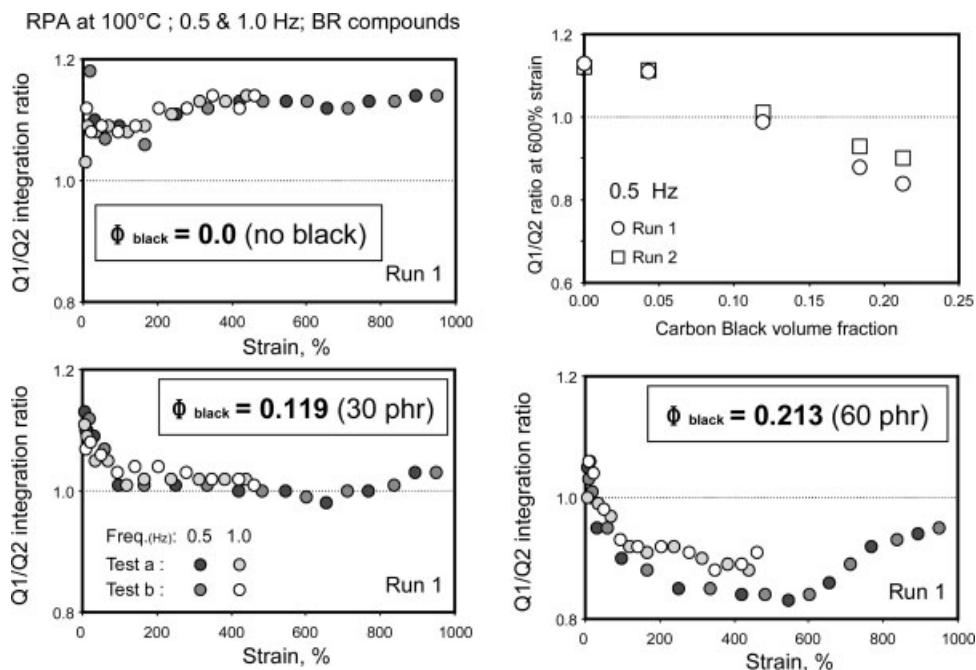


**Figure 17** Quarter cycle integration of averaged torque signal for polybutadiene compounds;  $Q1/Q2$  ratio at 600% strain documents the change from extra (strain-induced) to intra (morphology-induced) nonlinear viscoelastic character as filler content increases.

a sinusoidal strain, a clear distinction can be established between extra and intra nonlinear viscoelastic behaviors. The ratio of the first to the second quarter of integrated torque signal, i.e.,  $Q1/Q2$  allows to clearly distinguish between the strain amplitude effect on unfilled and filled materials, as shown in Figure 17 in the case of butadiene compounds. The unfilled material (upper left graph) exhibits a  $Q1/Q2$  ratio that is always higher than one and increases with strain amplitude; in such a case the torque signal is always distorted “on the left” (i.e.,  $Q1 > Q2$ ). One notes that the test frequency has no significant effect on  $Q1/Q2$ . With filled compounds,  $Q1/Q2$  is first higher than one a low strain, then quickly passes below one as  $\gamma$  increases, which correspond to a distortion “on the right” of the torque signal. If one considers the  $Q1/Q2$  ratio at a given strain, let’s say 600%, the change in nonlinear character as filler level increase is clearly illustrated (upper right graph in Fig. 17). Filled butadiene compounds change from extra to intra nonlinear behavior as filler content increases and, expectedly, the transition extra-to-intra occurs at a carbon black fraction that corresponds to the so-called percolation level (around 12–13% in volume fraction).

With respect to their filler loadings, all CEC composites exhibit essentially morphology-induced (or intra) nonlinear viscoelastic effects, as demonstrated by quarter cycle integration of torque signal. Figure 18 shows how the  $Q1/Q2$  ratio varies with strain amplitude for CEC samples, carbon black A series.

Run 1 data at 0.5 and 1.0 Hz are shown, without effect of test frequency. At low strain, the  $Q1/Q2$  ratio is slightly higher than or close to one for all the compounds investigated, then decreases with larger strain amplitude, reaches a minimum value before eventually increasing back towards one. Qualitatively, similar graphs are drawn with run 2 data but the minimum value is generally higher, at least for carbon black fractions below 0.270; in other words, the first strain sweep slightly reduces the intra nonlinearity, providing the filler content remains moderate. Similar graphs are drawn for the CEC samples, carbon black B series, with however some differences as explained below.

Figure 19 illustrates some interesting differences between the two series of CEC composites that can be assigned to the type of carbon black. As can be seen the lowest, the medium and the highest carbon black loaded compounds for the two series are illustrated. The difference between runs 1 and 2 is clearly seen for the moderate filler range (i.e., up to 0.270), as well as its disappearance for the highest loaded materials. The type of carbon black seems to affect the position of the minimum  $Q1/Q2$  ratio; for carbon black A composites, the minimum  $Q1/Q2$  clearly moves towards lower strain amplitude as filler content increases; for carbon black B composites, the minimum  $Q1/Q2$  ratio occurs at around 400% strain, irrespective of filler content. Carbon black A is a low specific surface area, high structure filler, while B is a high surface area, low structure carbon black.

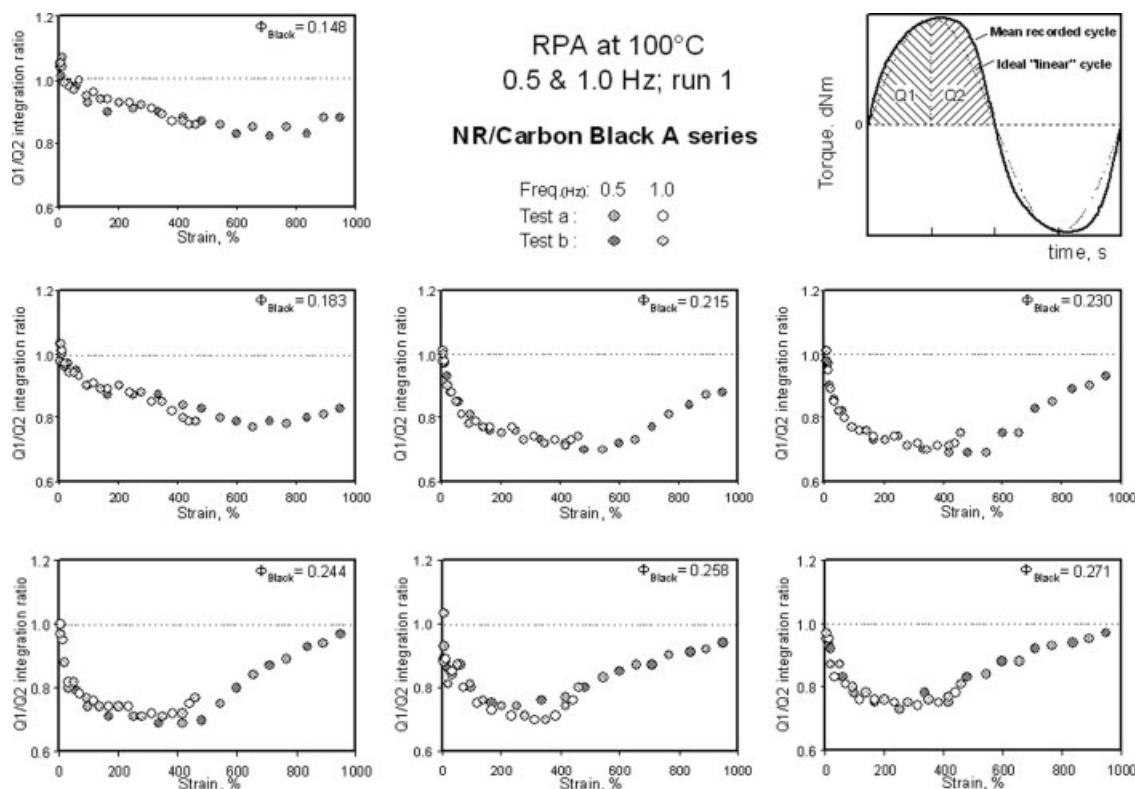


**Figure 18** Quarter cycle integration of averaged torque signal for CEC samples, carbon black A series; Run 1 data at 0.5 and 1.0 Hz

Quarter cycle integration and relative harmonics from FT are in fact two complementary manners to analyze the response of materials to periodic strains and therefore interpretation of both type of results must be very similar. Consequently, the position (on the strain scale) of the minimum  $Q1/Q2$  ratio could be considered as an indication of the maximum nonlinear effect due to the filler. A high structure filler would therefore be expected to offer a more complex nonlinear effect than a low structure one. However, two series of CEC composites with two different carbon blacks only cannot be considered as a sufficiently large sampling to strongly support this statement.

## CONCLUSIONS

Filled rubber compounds are complex polymer systems, which are conveniently characterized with advanced dynamic testing protocols developed for closed cavity rheometers. Using a purposely-modified closed cavity rheometer, strain sweep test protocols were performed on two series of NR/carbon black composites and a series of high *cis*-1,4 polybutadiene/carbon black compounds. Owing to their excessive stiffness in the molten state, highly filled

materials need special sample handling procedures to obtain reproducible results. Indeed, when closing the rheometer, radial flow is expected but hardly obtained with very stiff materials, despite the high axial compressive force used. A linear displacement transducer was fixed on the rheometer to document the actual cavity closure gap. Various experiments demonstrated that with stiff materials, not only the sample volume must be as close as possible to 110% of the empty cavity volume, but also that the actual shape of the sample is a relevant parameter. An appropriate sample preparation procedure was consequently developed, which proved to give very reproducible results.

Because nonlinear viscoelastic responses are obtained, results must be analyzed through special techniques, for instance the well-known Fourier Transform. FT spectra contain all the information available through dynamic testing and the nonlinear viscoelastic analysis was made by considering the main torque component  $T(\omega_1)$  and the relative harmonic torque components versus the strain amplitude. The main torque component gives access to the complex modulus, whose variation with strain amplitude was modeled with a simple four parameters equation. Fit model parameters provide quite interesting information on the viscoelastic behavior



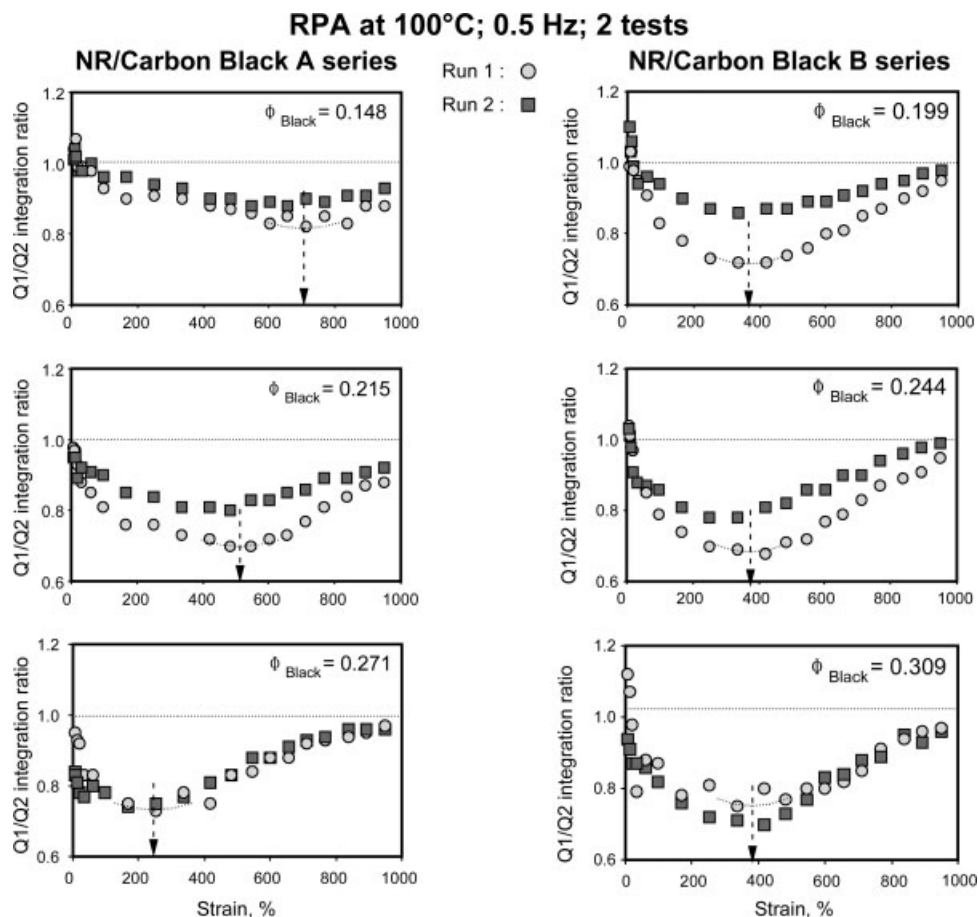


**Figure 19** Comparing  $Q1/Q2$  ratio versus strain amplitude for CEC samples, carbon black A and B series; run 1 and run 2 data at 0.5 Hz; the arrows indicates the approximate position of the minimum  $Q1/Q2$  ratio on the strain scale.

of filled rubber compounds, essentially affected by the filler content, with surprisingly relatively little effect of the matrix material, however limited to high *cis*-1,4 polybutadiene and natural rubber.

Odd torque harmonics become significant as strain increases and therefore the variation of torque harmonics with strain amplitude can be considered as the nonlinear viscoelastic “signature” of tested materials, only available through FT rheometry. If was found that, above a certain filler level, rubber compounds exhibit a typical pattern, with a “bump” appearing in the 500–600% strain range, essentially in total contrast with the features observed with either gum rubber or low filled compounds. With the hypothesis that this typical nonlinear viscoelastic “signature” reflects the superimposition of two responses, one common to all “pure” polymers and one expressing the filler contribution, a appropriate model equation was sought to fit experimental data.

The inspiration for an appropriate mathematical handling of the filler response was found in the failure modes analysis of industrial operations, with reference to the three parameters Weibull probability

density function. The logics behind the Weibull approach was transposed to the torque harmonics variation with strain magnitude of filled systems by considering that, because of strong interactions between the viscoelastic matrix and the discrete particles phase, a kind of soft composite network is embedded in the rubber phase. It results in additional harmonics in the medium strain range, which enhance the ongoing nonlinear response of the rubber matrix, then as strain further increases, filler-polymer interactions decrease and eventually vanish. With respect to such considerations, a suitable five parameters model was consequently developed and the strategy for nonlinear fitting it to experimental data was established. Excellent fit were obtained with the obvious advantage that large amounts of data are summarized in only five numbers whose magnitude can be analyzed with respect to test materials formulation. The filler loading appeared as the main factor affecting the nonlinear viscoelastic behavior, with minor effects due to the nature of the rubber matrix and the type of carbon black, while the sampling was not large enough to support strong conclusions in this regard.

Quarter cycle integration of (average) torque signal was found to provide additional information to FT analysis, with namely some results suggesting that the type of carbon black could affect the nonlinear viscoelastic response of filled compounds. Further works are needed to reinforce this conclusion.

The author would like to express his thanks to Dr. M.-J. Wang, from Cabot Corp. for his kindness and confidence in supplying the CEC samples used in this study.

#### APPENDIX: MODELING THE VARIATION OF COMPLEX MODULUS WITH STRAIN AMPLITUDE

Fitting experimental  $G^*$  versus strain data with a suitable mathematical model is an attractive manner to summarize large quantities of data, and the typical curves obtained allow a very fine analysis of this typical nonlinear behavior, providing model parameters receive a clear physical meaning. The model corresponds to eq. (A1):

$$G^*(\gamma_0) = G_f^* + \left[ \frac{G_0^* - G_f^*}{1 + (A\gamma_0)^B} \right] \quad (\text{A1})$$

where  $G_0^*$  is the modulus in the linear region,  $G_f^*$  the modulus for an infinite strain,  $A$  the reverse of a critical strain, which corresponds to  $(G_0^* + G_f^*)/2$ ,  $B$  a parameter describing the strain sensitivity of the material, and  $\gamma_0$  the strain amplitude (that we usually expressed in % strain). As shown in Figure A1, a  $G^*$  versus  $\gamma_0$  curve can be drawn with the equation and the inset parameters largely outside the experimental window. The modulus for an infinite strain  $G_f^*$  is a mere fitting parameter with obviously no physical meaning but  $G_0^*$ , the modulus in the linear region, can be considered as a true material parameter

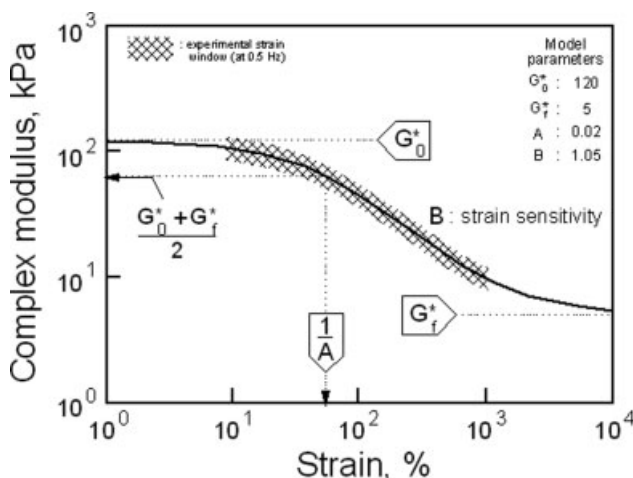


**Figure A1** Modeling  $G^*$  variation with strain amplitude; physical meaning of model parameters.

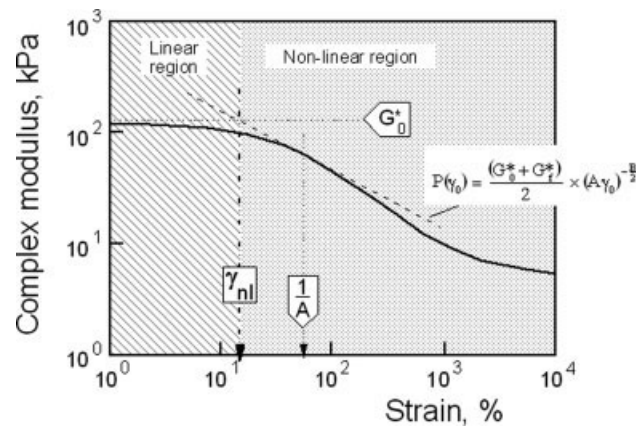


**Figure A2** Assessing the linear to nonlinear transition with  $G^*$  versus strain model parameters.

ter because one would indeed expect any virgin polymer to exhibit this behavior and also because a number of experimental results on gum rubbers really document the linear plateau (where the modulus is not depending on strain amplitude). The critical strain  $\frac{1}{A}$  corresponds to the mid modulus values between zero and infinite strain.  $B$  is called the strain sensitivity parameter because it affects the steepness of the curve in the nonlinear region.

By exploiting the mathematical virtues of eq. (A1), one can perform a very fine analysis of the nonlinear viscoelastic behavior. The first derivative of this equation allows to calculate the slope at any strain, i.e.

$$\text{Slope}(\gamma_0) = \frac{dG^*(\gamma_0)}{d\gamma_0} = \frac{(G_f^* - G_0^*)}{[1 + (A\gamma_0)^B]^2} \times (A\gamma_0)^B \times \frac{B}{\gamma_0} \quad (\text{A2})$$

Then, as illustrated in Figure A2, the straight line passing through point  $[(G_0^* + G_f^*)/2, 1/A]$  and having the slope calculated at  $\gamma_0 = \frac{1}{A}$  is of special interest because its intersection with the horizontal line corresponding to the linear modulus  $G_0^*$  provides a clear assessment of a critical strain  $\gamma_{nl}$  that could be considered as marking the transition from the linear to the nonlinear region. This line has the equation:  $P(\gamma_0) = [(G_0^* + G_f^*)/2] \times (A\gamma_0)^{-B}$  and the critical strain  $\gamma_{nl}$  is readily calculated with model parameters, as follows:

$$\gamma_{nl} = \frac{1}{A} \times \exp \left[ -2 \times \frac{\ln \left( 2 \times \frac{G_0^*}{G_0^* + G_f^*} \right)}{B} \right] \quad (\text{A3})$$

Using for instance model parameters values given in Figure A1, eq. (A3) yields  $\gamma_{nl} = 14.44\%$ . As shown in Figure A2, this critical strain is indeed well indicative of the linear to nonlinear transition.

## References

1. Wilhelm, M. *Macromol Mater Eng* 2002, 287, 83.
2. Leblanc, J. L.; de la Chapelle, C. *Rubber Chem Technol* 2003, 76, 979.
3. Leblanc, J. L. *Rubber Chem Technol* 2005, 78, 54.
4. Leblanc, J. L. *Ann Trans Nordic Rheol Soc* 2005, 13, 3.
5. Leblanc, J. L. *Rheol Acta* 2007, 46, 1013.
6. Friedrich, C.; Mattes, K.; Schulze, D. "Non-linear viscoelastic properties of polymer melts as analyzed by LAOS-FT experiments," IUPAC Macro 2004, Paris, France July 4–9, paper 6.1.3, 2004.
7. Neidhöfer, T.; Wilhelm, M.; Debbaut, B. *J Rheol* 2003, 47, 1351.
8. Schlatter, G.; Fleury, G.; Muller, R. *Macromolecules* 2005, 38, 6492.
9. CEC product data sheet; available at [www.cabot-corp.com](http://www.cabot-corp.com).
10. Wang, M.-J.; Wang, T.; Wong, Y. L.; Shell, J.; Mahmud, K. *Kautsch Gummi Kunstst* 2002, 55, 388.
11. Laube, S.; Shell, J. "Improving carcass durability through filler selection" Rubber Division Meeting, ACS, Savannah, GA, April 29–May 1, 2002, paper # 2.
12. Wang, T.; Wang, M.-J.; Shell, J.; Cabot, V. V.; Yao-Ling, F.; Guo-Qiang, F.; Jin, Z. *Rubber World* 2003, 227, 33.
13. Leblanc, J. L. *J Appl Polym Sci* 2006, 100, 5102.
14. Leblanc, J. L.; Mongruel, A. *Prog Rubber Plast Technol* 2001, 17, 162.
15. Guth, E.; Simha, R. *Kolloid-Zeitschrift* 1936, 74, 266.
16. Guth, E.; Gold, O. *Phys Rev* 1938, 53, 322.
17. Leblanc, J. L. *J Rubber Res* 2007, 10, 63.
18. Payne, A. R.; Whittaker, R. E. *Rubber Chem Technol* 1971, 44, 440.
19. Klüppel, M.; Heinrich, C. *Rubber Chem Technol* 1995, 68, 623.
20. Klüppel, M.; Schuster, R.; Heinrich, C. *Rubber Chem Technol* 1997, 70, 243.